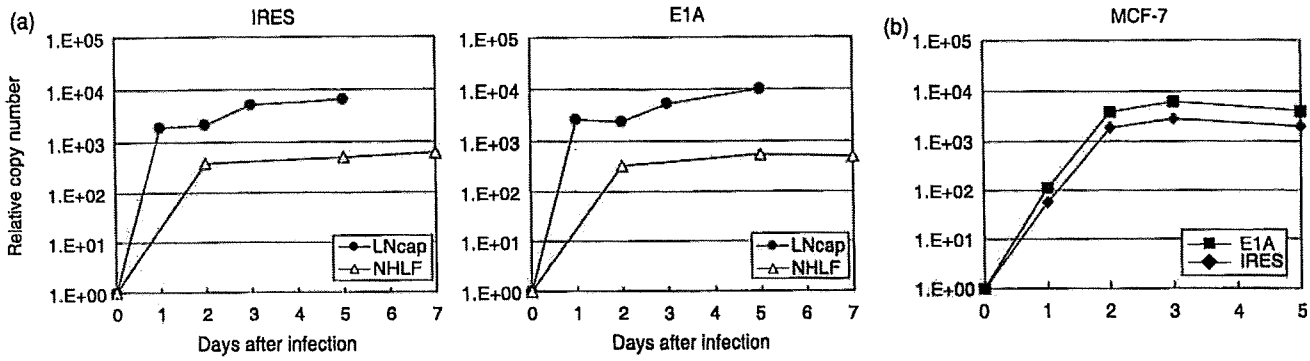

Fig. 4. Quantitative measurement of viral DNA replication in human cancer and normal cells *in vitro* by quantitative polymerase chain reaction (PCR) assay. (a) LNCap human prostate cancer cells and normal human lung fibroblast (NHLF) cells were infected with telomerase-specific replication-selective adenovirus (TRAD) at a multiplicity of infection (MOI) of 1 for 2 h. Following the removal of virus inoculum, cells were further incubated for the indicated periods of time, and then subjected to the real-time quantitative PCR assay. The amounts of viral internal ribosome entry site (IRES) and E1A copy number was defined as the fold increase for each sample relative to that at 2 h (2 h equals 1). (b) MCF-7 human breast cancer cells were infected with TRAD at a MOI of 1 and subjected to the PCR assay at the indicated time points. The relative TRAD DNA levels detected by IRES and E1A primers were plotted.

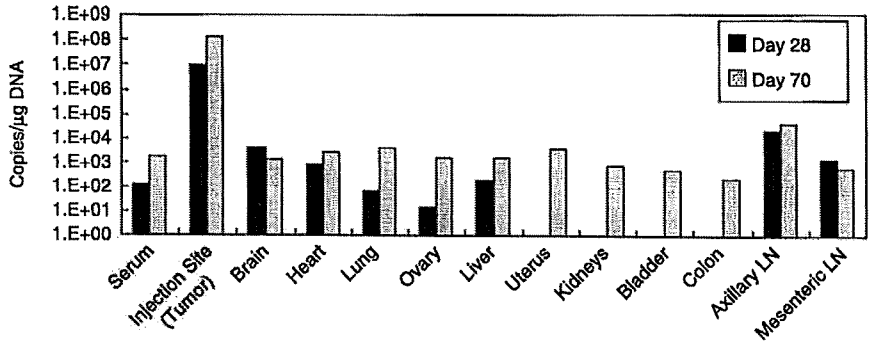

Fig. 5. Spread and replication of telomerase-specific replication-selective adenovirus (TRAD) following intratumoral administration in *nu/nμ* mice transplanted with A549 tumor cells. A549 tumor cells were injected subcutaneously into the right flank of mice at 5×10^6 cells/mouse. Mice received intratumoral injection of 1×10^8 plaque-forming units of TRAD when the tumor reached a size of approximately 5–6 mm in diameter. DNA was extracted from the subcutaneous tumor and various tissues of *nu/nμ* mice at 28 or 70 days after infection. Viral DNA was detected by quantitative polymerase chain reaction amplification of the adenoviral E1A sequence. The amounts of TRAD genome were defined as viral E1A copy number per μg DNA. LN, lymph nodes.

to avoid unexpected infectious disease due to viral overdose, we need assays that accurately detect the biological activity of viruses. In the present study, for clinical trials of TRAD, we developed an assay designed to estimate the biological activity of TRAD and to detect the copy number of TRAD in the plasma as well as tissues.

Although telomerase-specific TRAD exhibited a broad cytopathic effect against human cancer cell lines of different tissue origins, a human non-small-cell lung cancer cell line, H1299, was chosen for the biological assay of TRAD. H1299 was one of the most sensitive cell lines to TRAD-mediated cell death ($ID_{50} = 0.94$ MOI) and could be killed efficiently by TRAD infection in a dose-dependent fashion (Fig. 1). Because H1299 cells can be obtained from ATCC, they can be used in clinical laboratories to assess the biological activity of TRAD with a qualified standard protocol. In addition, although adenoviral E1B-55 kDa protein is known to bind to the tumor suppressor p53 protein,[12] H1299 cells are p53-null and therefore the interaction of E1B-55 kDa with p53, which in turn results in transcriptional modulation, can be ignored in this cell line. Thus, H1299 is considered an appropriate cell line for assessment of TRAD activity in certain preparations. In the present study, we considered TRAD to be active when the viability of H1299 cells was reduced by more than 50% at 48 h after TRAD infection at an MOI of 1. Using this biological assay, we confirmed that heat treatment of aliquots of TRAD at 56°C for 5 min is sufficient to inactivate its antitumor potential (Fig. 2c). These results advocate the use of the H1299 cell-based cytotoxicity assay as a standard method for quantitative assessment of the biological activity of TRAD in virus stocks for clinical trials.

Various biological methods, such as determination of infectious units in plaque assays, have been used routinely in clinical trials to monitor viral loads in the peripheral circulation.[8] These methods are useful for evaluating safety because the viral titers directly reflect the infectivity of viruses. However, because the plaque assay consists of labor-intensive and time-consuming steps, real-time monitoring of the biodistribution of the virus might be difficult. Here we described the development of a quantitative real-time PCR assay that can accurately quantify genome copy numbers of TRAD over a large linear range. Using primers targeting TRAD-specific sequences, such as adenoviral E1A and IRES, real-time PCR could accurately detect the number of TRAD genomes in the plasma as well as in the cells (Figs 3,4). The assay showed that TRAD replicated even in NHLF, although the level was much lower than that in tumor cells. It is usually difficult to maintain the normal cells primarily isolated from human tissues such as human hepatocytes in the culture; however, commercially available NHLF could be cultured for several passages, suggesting that NHLF may have some characteristics different from primary isolated normal cells, including

telomerase activity. We also found that the number of viral genomes could be measured in genomic DNA purified from tissues of mice *in vivo* after injection of TRAD into the xenografts (Fig. 5). Although viral DNA could be detected even in normal tissues 70 days after intratumoral injection of TRAD, the absence of infectious virus as assessed by the plaque assay suggests that there are only DNA fragments in tissues. Our preliminary experiments have demonstrated that DNA could be isolated from tumors as small as 5 mm in diameter (data not shown). Therefore, the real-time PCR method with E1A and IRES primers permits rapid and quantitative detection of TRAD DNA in clinical samples.

We have shown recently the antiviral activity of cidofovir against TRAD *in vitro*. Cidofovir is an acyclic nucleoside phosphonate with potent broad-spectrum anti-DNA viral activity and has been approved for the treatment of many types of viruses, including cytomegalovirus and adenovirus.[13] Although viremia after TRAD administration is extremely rare because of the anti-adenovirus antibodies expected to be present in most patients, a real-time PCR-based pharmacokinetic assay can allow the early detection of disseminated virus, and thus its use could provide an indication for commencement of cidofovir treatment in clinical trials.

In summary, we have established a fast, reliable, and sensitive assay to assess the biological activity of TRAD *in vitro* and to detect the viral genome in the plasma as well as tissues *in vivo*. A phase I clinical trial of TRAD targeting advanced solid tumors is currently underway in the USA following the approval of the Food and Drug Administration. Such an assay has been used in this ongoing trial and the data will be analyzed in the near future for the assessment of the safety, efficacy, and biodistribution of TRAD.

Acknowledgments

This work was supported in part by grants from the Ministry of Education, Science, and Culture, Japan, and by grants from the Ministry of Health and Welfare, Japan.

References

1 Kohn EC, Lu Y, Wang H *et al.* Molecular therapeutics: promise and challenges. *Semin Oncol* 2004; **31**: 39–53.
2 Hawkins LK, Lemoine NR, Kirn D. Oncolytic biotherapy: a novel therapeutic platform. *Lancet Oncol* 2002; **3**: 17–26.
3 Chiocca EA. Oncolytic viruses. *Nat Rev Cancer* 2002; **2**: 938–50.
4 Reid T, Galanis E, Abbruzzese J *et al.* Hepatic arterial infusion of a replication-selective oncolytic adenovirus (dl1520): phase II viral, immunologic, and clinical endpoints. *Cancer Res* 2002; **62**: 6070–9.
5 Hamid O, Varterasian ML, Wadler S *et al.* Phase II trial of intravenous CI-1042 in patients with metastatic colorectal cancer. *J Clin Oncol* 2003; **21**: 1498–504.
6 Kawashima T, Kagawa S, Kobayashi N *et al.* Telomerase-specific replication-selective virotherapy for human cancer. *Clin Cancer Res* 2004; **10**: 285–92.
7 Kim NW, Piatyszek MA, Prowse KR *et al.* Specific association of human telomerase activity with immortal cells and cancer. *Science* 1994; **266**: 2011–15.
8 Fujiwara T, Tanaka N, Kanazawa S *et al.* Multicenter phase I study of repeated intratumoral delivery of adenoviral p53 in patients with advanced non-small-cell lung cancer. *J Clin Oncol* 2006; **24**: 1689–99.
9 Umeoka T, Kawashima T, Kagawa S *et al.* Visualization of intrathoracically disseminated solid tumors in mice with optical imaging by telomerase-specific amplification of a transferred green fluorescent protein gene. *Cancer Res* 2004; **64**: 6259–65.
10 Taki M, Kagawa S, Nishizaki M *et al.* Enhanced oncolysis by a tropism-modified telomerase-specific replication-selective adenoviral agent OBP-405 ('Telomelysin-RGD'). *Oncogene* 2005; **24**: 3130–40.
11 Watanabe T, Hioki M, Fujiwara T *et al.* Histone deacetylase inhibitor FR901228 enhances the antitumor effect of telomerase-specific replication-selective adenoviral agent TRAD in human lung cancer cells. *Exp Cell Res* 2006; **312**: 256–65.
12 Cathomen T, Weitzman MD. A functional complex of adenovirus proteins E1B-55kDa and E4orf6 is necessary to modulate the expression level of p53 but not its transcriptional activity. *J Virol* 2000; **74**: 11 407–12.
13 Ouchi M, Kawamura H, Nagai K, Urata Y, Fujiwara T. Antiviral activity of cidofovir against telomerase-specific replication-competent adenovirus, Telomelysin (OBP-301). *Mol Ther* 2007; **15** (Suppl 1): S173.

doi: 10.1111/j.1349-7006.2007.00665.x

Int. J. Cancer: **122,** 2628–2633 (2008)

Combination of oncolytic adenovirotherapy and Bax gene therapy in human cancer xenografted models. Potential merits and hurdles for combination therapy

Masayoshi Hioki[1,2], Shunsuke Kagawa[1,2]*, Toshiya Fujiwara[1,2], Ryo Sakai[1,2], Toru Kojima[1,2], Yuichi Watanabe[1,3], Yuuri Hashimoto[3], Futoshi Uno[1,2], Noriaki Tanaka[1] and Toshiyoshi Fujiwara[1,2]

[1]*Division of Surgical Oncology, Department of Surgery, Okayama University Graduate School of Medicine, Dentistry and Pharmaceutical Sciences, 2-5-1 Shikata-cho, Okayama 700-8558, Japan*
[2]*Center for Gene and Cell Therapy, Okayama University Hospital, Okayama, Japan*
[3]*Oncolys BioPharma, Inc., Tokyo, Japan*

Cancer gene therapy and oncolytic virotherapy have been studied extensively. However, their clinical application is hampered by their weak anticancer activity. We previously constructed a replicating adenovirus (OBP-301, Telomelysin), in which the human telomerase reverse transcriptase (hTERT) promoter drives expression of the adenoviral E1 genes, and causes selective lysis of human cancer cells. We hypothesized that combination adenoviral therapy containing OBP-301 and a nonreplicating adenovirus expressing the proapoptotic Bax gene could overcome the weakness and augment the anticancer efficacy of each modality. Combination treatment resulted in marked Bax protein expression and enhanced efficacy in *in vitro* cell viability assay, when compared with either single treatment. However, combination treatment was not as effective in suppressing both subcutaneous and pleural disseminated tumors compared with OBP-301 treatment alone. Further investigation revealed that combination treatment resulted in suppressed E1A protein expression associated with reduced viral replication. Our results suggest that Bax gene therapy in combination with oncolytic adenovirotherapy potentially augments their antitumor activity, but further improvements may be required to maximize the combinatorial effect *in vivo*, for the Bax gene expression to avoid interference with production of the oncolytic virus.

Key words: gene therapy; oncolytic virus; bax; adenovirus

Oncolytic adenoviruses that can selectively replicate in tumor cells and cause lysis of infected cells have been extensively investigated as novel anticancer agents.[1,2] Recently, such vectors have been approved for clinical trials.[3–8] However, preclinical and clinical studies have revealed that the clinical application of these agents is hampered by their weak anticancer activity. Therefore, the development of strategies that maximize their anticancer activity is essential to the success of these agents in treating cancer.

One of the approaches to overcome this weakness is combination therapy of the oncolytic virus with a virus expressing therapeutic genes such as proapoptotic genes to augment the killing effect on cancer cells, which may lead to the future development of an arming oncolytic virus as a cancer therapeutic.

Bax is a strong proapoptotic gene that causes cytochrome C release from mitochondria, activates the caspase pathway and leads to apoptosis.[9,10] We previously constructed a binary adenoviral vector system (Ad/PGK-GV16 + Ad/GT-Bax: Ad/Bax) for Bax overexpression[11] that can transfer the Bax gene to cancer cells *in vitro* and *in vivo* and induce effective apoptosis.[12,13] However, because this system consists of E1-deleted, replication-defective adenovirus, its cell killing activity is theoretically limited to the transduced cells.

We also constructed a novel oncolytic adenovirus (OBP-301, Telomelysin), in which the human telomerase reverse transcriptase (hTERT) promoter drives expression of the adenoviral E1 genes. OBP-301 thus replicates preferentially in human cancer cells and causes their selective lysis.[14] However, as this virus also does not contain any therapeutic genes, clinical weakness is anticipated.

We hypothesize that Bax gene therapy in combination with an onlytic adenovirus could augment anticancer efficacy by overcoming the weakness of each modality. The replication-defective adenovirus with E1 deletion can become replication-competent when cotransduced with an oncolytic adenovirus supplying E1 *in trans*. Thus, the expression of the Bax gene and the viral copies would increase, which facilitates cancer cells to undergo apoptosis, release virus progenies and further spread them within the tumor.

In this study, we evaluated the transgene expression, viral replication and antitumor effect of Bax gene therapy combined with OBP-301 oncolytic adenovirotherapy in human cancer cell lines.

Material and methods

Cell lines and cell culture

Human bronchioloalveolar carcinoma A549 cells were propagated in a monolayer culture in Dulbecco's modified Eagle's medium containing Ham's F-12 nutrient mixture supplemented with 10% fetal calf serum (FCS) and antibiotics. Human gastric cancer MKN45 cells were cultured in RPMI 1640 medium containing 10% FCS and antibiotics. The cells were cultured at 37°C in a humidified incubator containing 5% CO_2.

Recombinant adenoviruses

The recombinant replication-selective, tumor-specific adenovirus vector OBP-301 (Telomelysin), and nonreplicating E1-deleted binary adenovirus vector system expressing the proapoptotic Bax gene (Ad/PGK-GV16 + Ad/GT-Bax: Ad/Bax) were previously constructed and characterized.[11,14] In a binary vector system, expression of the *Bax* gene can be induced by transferring Ad/GT-Bax into target cells along with Ad/PGK-GV16 at a ratio of 1:1. All of the viruses were propagated in a package containing 293 cells and purified by $CsCl_2$ step gradient ultracentrifugation followed by $CsCl_2$ linear gradient ultracentrifugation. Determination of virus particle titer and infectious titer (plaque-forming unit: PFU) was accomplished spectrophotometrically by the method of Maizel *et al.*[15] and by the method of Kanegae *et al.*,[16] respectively. The particles: plaque ratios were between 23:1 and 35:1.

Cell viability assay

Cells were plated in 96-well plates at a density of 1,000 cells/well and infected with OBP-301 alone, Ad/Bax alone, or their combination 15 hr later. Cell viability was assessed using a colorimetric XTT assay with the Cell Proliferation Kit II (Roche Molecular Biochemicals, Indianapolis, IN) according to the manufacturer's protocol. We determined the combination index (CI) at

This article contains supplementary material available via the Internet at http://www.interscience.wiley.com/jpages/0020-7136/suppmat.

Grant sponsors: Ministry of Education, Culture, Sports, Science and Technology of Japan, Ministry of Health, Labour and Welfare of Japan.

*Correspondence to: Center for Gene and Cell Therapy, Okayama University Hospital, 2-5-1 Shikata-cho, Okayama 700-8558, Japan. Fax: +81-86-235-7884. E-mail: skagawa@md.okayama-u.ac.jp

Received 8 May 2007; Accepted after revision 5 December 2007
DOI 10.1002/ijc.23438
Published online 13 March 2008 in Wiley InterScience (www.interscience.wiley.com).

different multiplicities of infection (MOIs) in A549 cells with CalcuSyn software (BioSoft, Cambridge, UK).

Cell cycle analysis

A549 and MKN45 cells were seeded on 6-well plates at 1×10^5 cells/well and were infected with OBP-301 at an MOI of 1 PFU/cell, Ad/Bax at an MOI of 5 or 50 PFU/cell, or OBP-301 at an MOI of 1 PFU/cell in combination with Ad/Bax at an MOI of 5 PFU/cell 15 hr later. At 24 and 96 hr after infection, adherent cells were harvested with trypsin-EDTA and nonadherent cells were also harvested. All cells were washed with PBS, fixed and permeated with 70% ice-cold ethanol at 4°C for 12 h. Cells were centrifuged at 1,200 rpm, resuspended in freshly prepared propidium iodide (PI) staining buffer (0.1% Triton X-100, 200 μg/ml RNase, and 50 μg/ml PI in PBS), and incubated for 30 min at 4°C in the dark. Single color fluorescent flow cytometry was performed with a FACS calibur flow cytometer (Becton Dickinson, San Jose, CA). The histograms were analyzed with FlowJO software (Tree Star, Ashland, OR).

Western blot analysis

A549 cells were seeded and infected with OBP-301 alone, Ad/Bax alone, or their combination at an MOI of 1 PFU/cell 15 hr later. The cells were incubated at 37°C and harvested for Western blot analysis at 72 and 120 hr. The primary antibodies against Bax (Santa Cruz Biotechnology, Santa Cruz, CA), caspase 3, E1A (BD Biosciences, San Jose, CA) and β-actin (Sigma, St. Louis, MO) and peroxidase-linked secondary antibody (Amersham, Arlington Heights IL) were used. Cells were washed twice in cold PBS, collected and lysed in lysis buffer [10 mM Tris (pH 7.5), 150 mM NaCl, 50 mM NaF, 1 mM EDTA, 10% glycerol, 0.5% NP40] containing proteinase inhibitors (0.1 mM phenylmethylsulfonyl fluoride, 0.5 mM Na3VO4). After 20 min on ice, the lysates were spun at 14,000 rpm at 4°C for 10 min. The supernatants were used as whole cell extracts. Protein concentration was determined using the Bio-Rad protein determination method (Bio-Rad, Richmond, CA). Equal amounts of proteins were boiled for 5 min and electrophoresed under reducing conditions on 4–12% (w/v) polyacrylamide gels. Proteins were electrophoretically transferred to Hybond polyvinylidene difluoride transfer membranes (Amersham Life Science, Buckinghamshire, UK) and incubated with the primary followed by peroxidase-linked secondary antibody. An ECL chemiluminescent Western blot system (Amersham) was used to detect secondary probes.

Animal experiments

A549 xenografts were established in 6-week-old female nude mice (Balb/c nu/nu) through subcutaneous inoculation of 2×10^6 A549 cells into the dorsal flank. Once each tumor reached a diameter of ~3–9 mm, the mice were randomly assigned into 4 groups and a 50-μl solution containing OBP-301, Ad/Bax, or their combination, at a dose of 1×10^7 PFU/body or PBS was injected into the tumor on 3 consecutive days. Tumors were measured 2–3 times a week and tumor volume was calculated using the equation $a \times b^2 \times 0.5$, in which a and b are the largest and smallest diameters, respectively. Animals were killed when their tumor reached a diameter of ~15 mm. To develop pleural disseminated xenografts, mice were inoculated with 2×10^6 A549 cells into the pleural cavity through a 27-gauge needle. Also, to assess the efficiency of adenoviral gene transfer into the pleural disseminated tumors, 24 hr after tumor injection, 100 μl of 1.0×10^7 PFU of OBP-301, Ad/Bax, both of them, or PBS was injected into the thoracic space by the same technique. The procedure was repeated over 3 consecutive days. Three weeks after cell inoculation, the mice were killed and their thoracic spaces were examined macroscopically for any growths. Tumors in the thoracic spaces were removed and weighed. The experimental protocol was approved by the Ethics Review Committee for Animal Experimentation of Okayama University School of Medicine, Okayama, Japan. The tumor growth of each group was statistically analyzed by Student t-test and a p-value of ≤ 0.05 was considered significant.

Viral replication assay in vivo

A549 cells were injected into the dorsal flank of nude mice. When the tumor reached a size of ~5 mm, 1×10^7 PFU of OBP-301, OBP-301 + Ad/Bax, OBP-301 + Ad/LacZ, or Ad/Bax was injected to the tumors ($n = 5$, each group). Tumors were harvested 7 days after viral injection, immediately frozen and milled in PBS by using Micro Smash MS-100 (Tomy Digital Biology, Tokyo, Japan). The virus was then extracted by freezing and thawing 3 times and cell debris was spun down. The supernatant was collected and subjected to titer assay for viral PFU. The final result was expressed as a total PFU from 1 whole tumor.

Quantitative real-time polymerase chain reaction

A549 cells were seeded on 25-cm^2 flasks at 5×10^5 cells 15 hr before infection. Cells were infected with OBP-301 alone or in combination with Ad/Bax or Ad/lacZ 15 hr later. The cells were incubated at 37°C, trypsinized and harvested for replication analysis at 48 hr. DNA purification was performed using a QIAmp DNA mini kit (Qiagen, Valencia, CA). The E1A DNA copy number was determined by quantitative real time polymerase chain reaction (PCR), using a LightCycler instrument and LightCycler-DNA Master SYBR Green I (Roche Diagnostics).

Results

Combination of oncolytic virotherapy and Bax gene therapy enhanced cell killing in vitro

To compare the efficacy of the combined use of oncolytic virotherapy with Bax gene therapy *in vitro*, A549 and MKN45 human cancer cells were treated with OBP-301 alone, Ad/Bax alone, or the combination. Based on each optimal condition, A549 was infected with OBP-301 at 1 MOI and Ad/Bax at 10 MOI, and MKN45 was infected at 10 MOI in both viruses. In both cell lines, Ad/Bax treatment showed only minimal suppression of cell viability and OBP-301 treatment showed a modest and delayed oncolytic effect, whereas combination treatment with OBP-301 and Ad/Bax induced rapid and massive cell death, and almost complete cell killing (Fig. 1).

To evaluate the synergistic effect of the combined oncolytic virotherapy and Bax gene therapy, the CI was determined at different MOIs (Table I) with CalcuSyn software (BioSoft, Cambridge, UK). We found that in A549 cells, the combination of OBP-301 with Ad/Bax led to a strong synergism (CI < 0.3).

Bax gene therapy in combination with oncolytic virotherapy increased the production of Bax protein in vitro *and induction of apoptosis*

To examine Bax protein expression in cells infected with the replication-deficient Ad/Bax in combination with the replicating OBP-301, A549 cells were infected with OBP-301 alone, Ad/Bax alone, or OBP-301 in combination with Ad/Bax or Ad/lacZ and then harvested on day 3 or 5. Cells treated with OBP-301 or the combination of OBP-301 with Ad/lacZ resulted in minimal Bax protein expression, whereas treatment with Ad/Bax and the combination treatment with OBP-301 plus Ad/Bax showed higher expression of Bax protein. Densitometric measurement documented increments of Bax expression by combination of Ad/Bax with OBP-301 (Fig. 2). In addition, treatment with OBP-301 plus Ad/Bax resulted in caspase-3 activation, while treatment with OBP-301 only or OBP-301 plus control virus Ad/lacZ did not. This means that the combination with Ad/Bax activates the apoptotic cascade in cancer cells cotreated with oncolytic virus.

Bax gene therapy in combination with oncolytic virotherapy increased apoptotic cells in vitro

To quantify the apoptotic effects of Ad/Bax treatment in combination with OBP-301 treatment, sub-G1/G0 fractions were

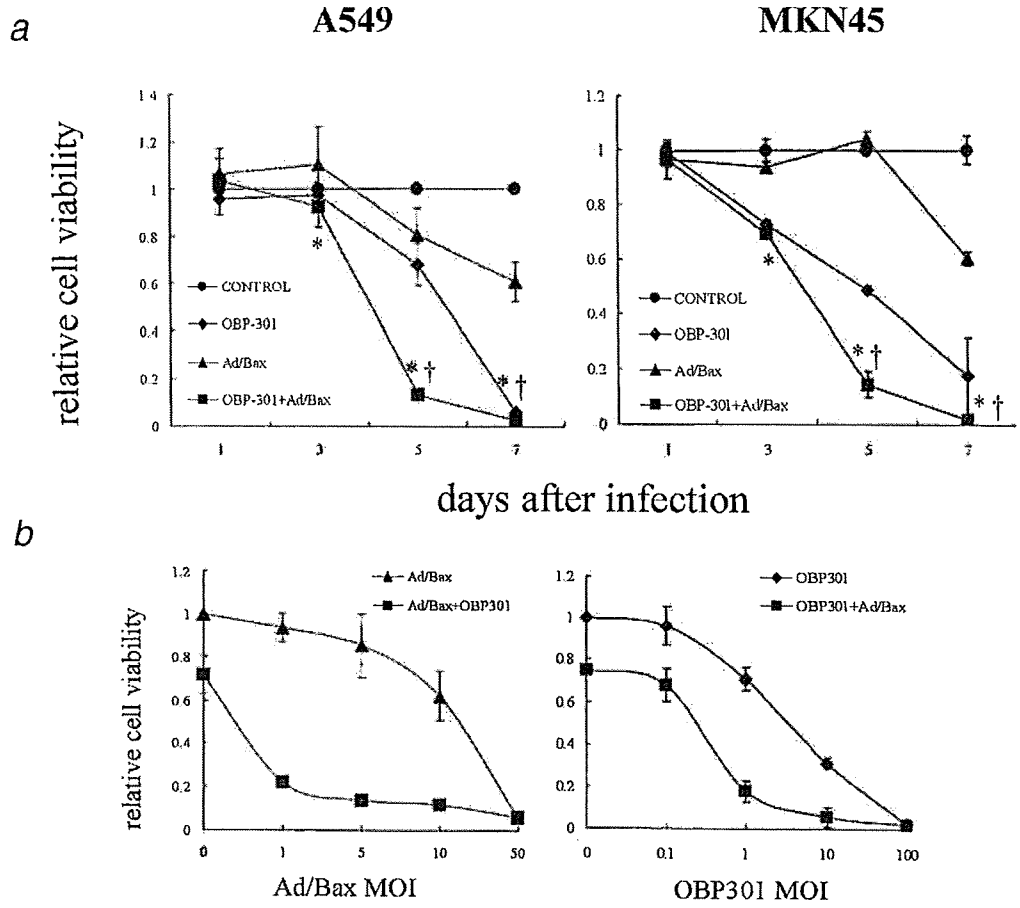

FIGURE 1 – Cytotoxity effects of OBP-301 combined with Ad/Bax in human cancer cell lines. (*a*) The indicated cancer cells were infected with OBP-301 alone, Ad/Bax alone, or in combination at the indicated MOI. Cell viability was assessed by XTT assay over 7 days. Bars, standard deviation (SD). *, $p < 0.05$, OBP-301 + Ad/Bax versus Ad/Bax alone; †, $p < 0.05$, OBP-301 + Ad/Bax versus OBP-301 alone. (*b*) A549 cells were infected with 1 MOI of OBP-301 and Ad/Bax at the indicated MOI (left), or 10 MOI of Ad/Bax and OBP-301 at the indicated MOI (right). Cell viability was assessed by XTT assay at 5 days after infection. Bars, SD.

TABLE I – COMBINATION INDEX (CI) OF OBP-301 AND Ad/Bax

Ad/Bax (MOI)	CI
1	0.122
5	0.111
10	0.132
50	0.217
OBP301 (MOI)	**CI**
0.1	1.054
1	0.144
10	0.197
100	0.592

determined by flow cytometry. A549 cells were infected with OBP-301, Ad/Bax, or OBP-301 plus Ad/Bax, and then subjected to the analysis at day 4. Although treatment with OBP-301 or Ad/Bax resulted in only background levels of apoptotic cells similar to that of mock infection, treatment with Ad/Bax plus OBP-301 markedly increased the apoptotic cells (Fig. 3).

Combination with Bax gene therapy did not augment antitumor activity of OBP-301-mediated oncolytic virotherapy in vivo

Based on the *in vitro* favorable combination effect of Ad/Bax and OBP-301, the antitumor effect on established tumors was further assessed. The A549 tumors were established in the dorsal

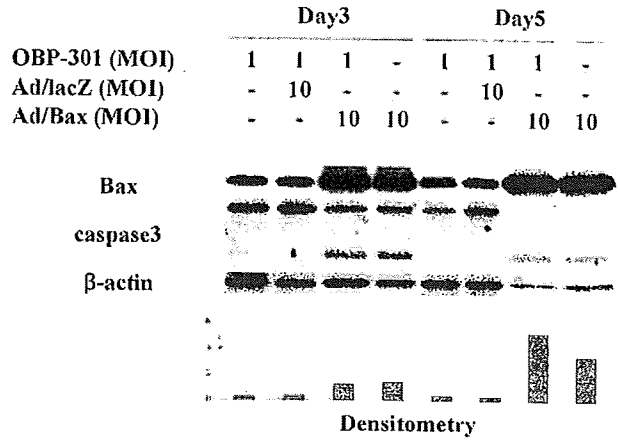

FIGURE 2 – Expression of Bax and caspase 3 in cells infected with Ad/Bax in combination with OBP-301. A549 cells were infected at 1 MOI of OBP-301 alone, 10 MOI of Ad/Bax alone, or 1 MOI of OBP-301 in combination with 10 MOI of Ad/Bax or Ad/lacZ, and then harvested at day 3 or 5. Lysates were subjected to immunoblot analysis with antibodies recognizing Bax, caspase 3, or β-actin. The lower panel shows the intensity of each band of Bax determined by densitometric scanning using NIH image software and normalized by dividing the actin signal.

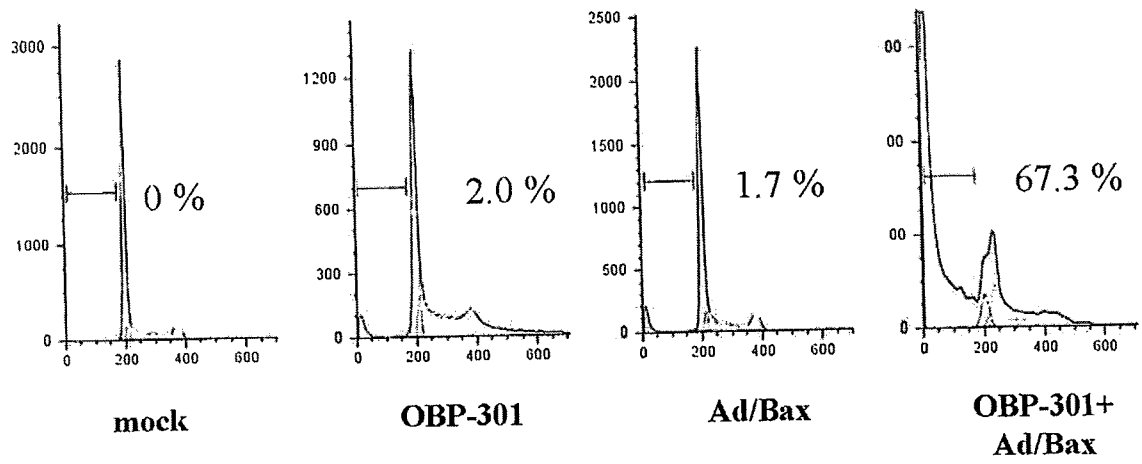

FIGURE 3 – Cell cycle analysis in A549 cells infected with OBP-301 in combination with Ad/Bax. Indicated cancer cells were infected with mock solution, 1 MOI of OBP-301, 10 MOI of Ad/Bax, or 1 MOI of OBP-301 plus 10 MOI of Ad/Bax, and harvested at day 4; cell cycle analysis using flow cytometry was then performed. The histograms were analyzed with FlowJO software.

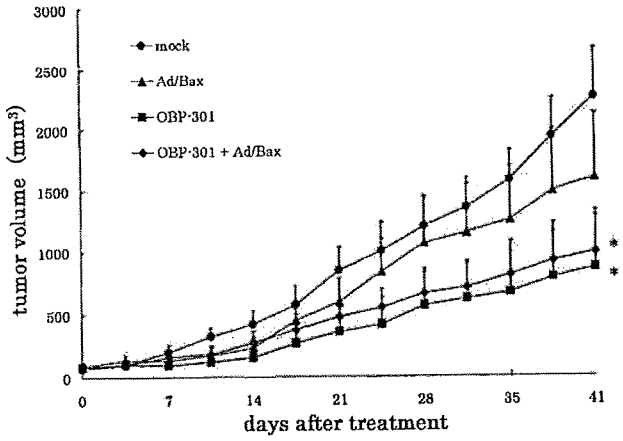

FIGURE 4 – Tumor xenograft size after infection with OBP-301, Ad/Bax, or their combination. A549 xenografts were established in nude mice (Balb/c nu/nu) through subcutaneous inoculation of 2×10^6 A549 cells into the dorsal flank. When the tumor reached a diameter of ~5 mm, the virus solution was injected into the tumor at a dose of 1×10^7 PFU/body on 3 consecutive days. Tumor volume was calculated using the equation $a \times b^2 \times 0.5$, in which a and b are the largest and smallest diameters, respectively. Bars, standard error (SE). *, $p < 0.05$, compared with mock-treated tumors.

flank of nude mice and the virus was injected into the tumor at a dose of 1×10^7 PFU/body on 3 consecutive days. Tumor size was measured 2–3 times a week and followed for up to 41 days. Treatment with Ad/Bax alone did not suppressed tumor growth significantly when compared with mock treatment because of a suboptimal dose, whereas treatments with OBP-301 and OBP-301 plus Ad/Bax significantly suppressed tumor growth when compared with other controls ($p \leq 0.05$; Fig. 4). However, the effect of adding Ad/Bax to OBP-301 treatment was less than expected, and the difference was not significant.

We also examined the antitumor effects of this combination treatment in mice with pleurally disseminated A549 tumors. The mice were injected with 100 μl of 1.0×10^7 PFU of OBP-301, Ad/Bax, or both into the thoracic space on 3 consecutive days. Three weeks after cell inoculation, the mice were killed and their thoracic spaces were examined macroscopically for any growths. To quantitate the reduction of tumor burden in the thoracic spaces, the tumors were removed and weighed. Although treatment with OBP-301 alone or Ad/Bax in combination with OBP-301 significantly suppressed tumor weight, there was no significant difference between them (Figs. 5*a* and 5*b*). These results suggest that Bax gene therapy does not augment oncolytic virotherapy *in vivo*.

Combination treatment resulted in suppressed E1A protein expression due to reduced viral replication in vitro

To explore the underlying mechanism by which oncolytic virotherapy did not work cooperatively with proapoptotic Bax gene therapy, E1A protein expression was examined by Western blot analysis. A549 cells were treated with each virus singly or in combination and then subjected to the analysis at days 3 and 5. Treatment with OBP-301 alone and in combination treatment with Ad/lacZ demonstrated increased E1A protein expression, meaning efficient viral replication. Treatment with Ad/Bax alone showed no E1A protein expression because of the E1-deficient replication incompetent virus. Of note, treatment with OBP-301 plus Ad/Bax showed suppressed expression of E1A protein when compared with treatment with OBP-301 alone, meaning that the combination with Ad/Bax may interfere with viral replication (Fig. 6).

To further document the effect of Bax expression on the process of viral propagation, the replication and release of viral progenies were measured by quantitative real time PCR. A549 cells were infected with viruses and the supernatants of the cell groups were collected. DNA was extracted from them and subjected to the assay. We found suppressed viral copy numbers in cells treated with the combinations with Ad/Bax and Ad/lacZ (Fig. 7). The inhibition of E1A copy numbers in a group of Ad/Bax combination was about 10 times of inhibition in a group of Ad/lacZ combination. Our results suggest that Bax gene therapy may interfere with viral production and thus be not conducive to oncolytic virotherapy. To further examine viral replication *in vivo*, the amounts of infectious viruses produced in the tumors were analyzed. Titers were very low for tumors treated with Ad/Bax because of a lack of replication in the absence of E1 gene, while tumors treated with OBP-301 produced higher amount of infectious virus than those treated with Ad/Bax alone, suggesting viral replication in tumors. However, because of the large variation in data from each group, there was no significant difference between treatment groups (data not shown).

Discussion

Replication-competent oncolytic adenovirus has shown a remarkable safety profile but efficacy for cancer therapy continues to be a major obstacle. To eliminate cancer cells, the virus also must spread throughout the bulk of the tumor and induce cell

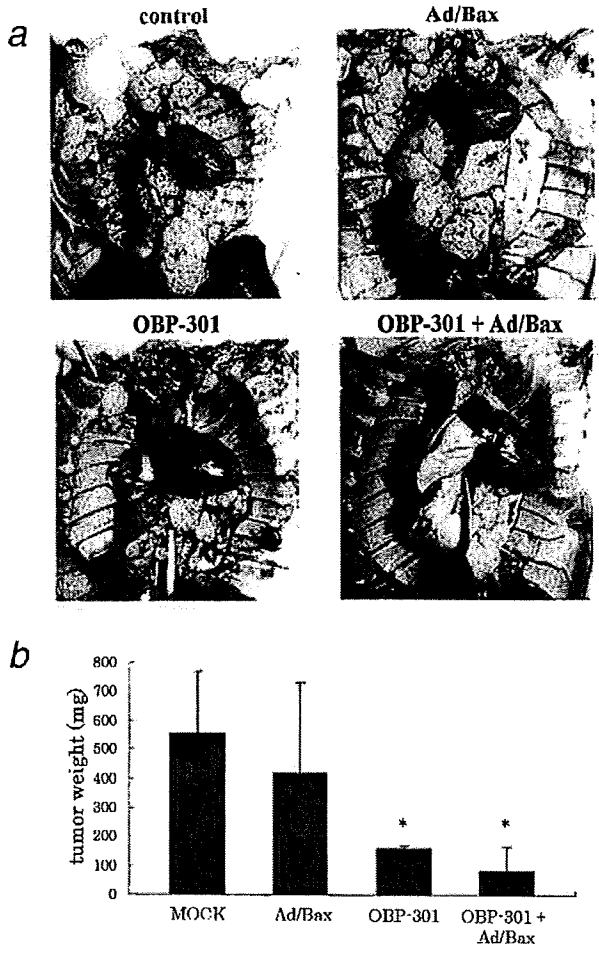

FIGURE 5 – Antitumor effects of OBP-301 combined with Ad/Bax in mice with A549 pleural dissemination. Mice were inoculated with 2×10^6 A549 cells into the pleural cavity, and 24 hr after tumor injection, 100 μl of 1.0×10^7 PFU of OBP-301, Ad/Bax, both of them, or PBS was injected into the thoracic space. The procedure was repeated over 3 consecutive days. (*a*) Three weeks after cell inoculation, mice were killed and their thoracic spaces were examined macroscopically for any growths. (*b*) Tumors in the thoracic spaces were removed and weighed. Bars, SD. *, $p < 0.05$, compared with mock-treated tumors.

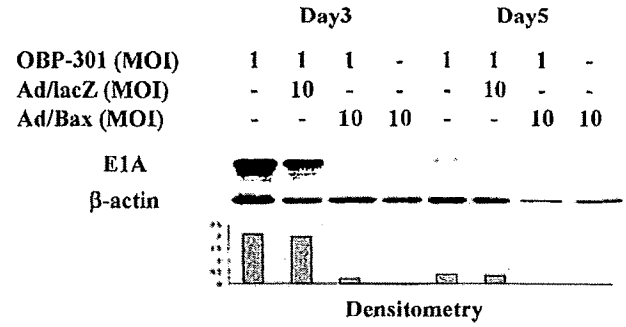

FIGURE 6 – Expression of E1A in cells infected with Ad/Bax in combination with OBP-301. A549 cells were infected at 1 MOI of OBP-301 alone, 10 MOI of Ad/Bax alone, or 1 MOI of OBP-301 in combination with 10 MOI of Ad/Bax or Ad/lacZ, and then harvested at day 3 or 5. Lysates were subjected to immunoblot analysis with antibodies recognizing E1A or β-actin. The lower panel shows the intensity of each band of Bax determined by densitometric scanning using NIH image software and normalized by dividing the actin signal.

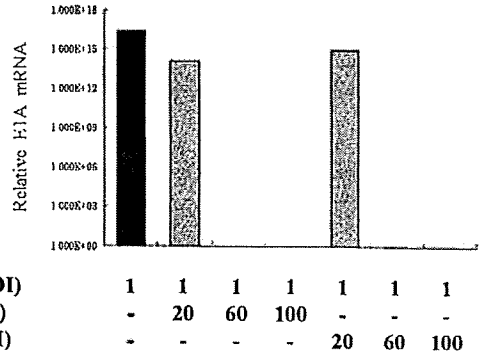

FIGURE 7 – Assessment of viral DNA replication in cells infected with Ad/Bax in combination with OBP-301. A549 cells were seeded on 25-cm^2 flasks at 5×10^5 cells 15 hr before infection. Cells were infected with OBP-301 alone, Ad/Bax alone, or their combination at an MOI of 1 PFU/cell 15 hr later. The cells were harvested at 48 hr and then subjected to real-time quantitative PCR assay. The amounts of viral E1A copy number are defined as the fold increase for each sample relative to that at 2 hr (2 hr equals 1).

death. Even with replicating adenoviral systems, the necessity to infect all cancer cells remains a major challenge.

In this study, we hypothesized that the oncolytic adenovirotherapy combined with Bax gene therapy could enhance the oncolytic potency. As expected, the combination treatment resulted in Bax overexpression, induced early apoptosis and enhanced efficacy in the cell viability assay *in vitro*. However, disappointingly, combination treatment did not result in further reductions in flank tumor size and pleural disseminated tumor weight, which was associated with suppressed E1A protein expression and reduced viral replication of OBP-301.

The antitumor effect of the oncolytic virus depends on the cytopathic effect intrinsic to adenovirus replication and dissemination throughout the tumor mass. Because viral infection of the tumor bulk depends on cell-to-cell viral spread, there may be a race between rapid tumor growth and viral spread. Therefore, to improve the efficacy of oncolytic virotherapy, the accelerated viral release and induction of cell death must be necessary. A previous study has shown that loss of E1b-19kD function in a replicating adenovirus enhances early viral release, leading to accelerated cell-to-cell viral spread.[17] In turn, Chiou and White reported that inhibition of apoptosis could severely attenuate viral release.[18] Taken together, this suggests that a combination of proapoptotic gene therapy and oncolytic virotherapy may improve the antitumor efficacy by enhancing cell-to-cell spread of the virus. The other rationale of the combination of proapoptotic gene therapy is to cope with the cancer resistance to the oncolytic virotherapy. Because heterogeneity in cancer cell populations drives the development of resistance, the approach of killing cells by multiple nonoverlapping mechanisms could be a solution. Although an oncolytic virus can kill cells by apoptosis-independent mechanisms such as direct cell lysis and necrosis, cells treated with combination therapy showed a pattern of apoptosis evidenced by analysis of the cell cycle. However, because induction of apoptosis and premature cell lysis may potentially compromise viral yield, reduced viral production could be a concern in using Bax-expressing virus in combination.

In the *in vitro* cell viability assay, the combination of Bax-expressing adenovirus with a replicating adenovirus leads to increased apoptosis at an earlier phase as theoretically anticipated. In turn, we have demonstrated a reduced viral yield in A549 cells. The early apoptotic cell death induced by Bax overexpression may limit an increase of virus and disturb viral replication. Our results are consistent with those of Lambright *et al.*,[19] who found that the addition of ganciclovir therapy to a replicating vector containing the HSVtk suicide gene did not augment efficacy, despite the enhanced production of the transgene. Viral replication and timely cell-death induction thus need to be well coordinated, and forced

induction of early apoptosis could be a cause of losing the combinative effect. Our data suggest that impaired viral replication may offset the benefits due to enhanced transgene spread *in vivo*.

In this study, we have shown the discrepancy between *in vitro* and *in vivo* findings, but this would not result solely from the reduced viral replication. Although viruses can rapidly and evenly spread in cell culture monolayer, this would not be expected in a solid tumor. In a tumor mass, it is very difficult to distribute viral progenies to even the majority of tumor cells. Because a cancer-targeting oncolytic virus is designed to selectively replicate in cancer cells, the normal interstitial cells would be obstacles. The virus would also face other obstacles for viral distribution, including tight intercellular space and continuous drainage by the circulatory and lymphatic systems. In this circumstance, the intratumoral dispersion is confined to one part of the tumor, and thus the requirement of double infection in a complementary strategy curtails the efficacy at low multiplicities of infection.

Although our data suggest that Bax gene therapy in combination with oncolytic adenovirotherapy is not likely to be therapeutically beneficial, the concept of "armed" replicating adenovirotherapy still has potential merit. Overexpression of the adenoviral death protein, expression of TRAIL and deletion of the E1B-19kD gene have all been shown to improve viral spread and efficacy of replicating adenoviruses *in vitro* and *in vivo*.[5,17,20–25] Various suicide genes or cytokines have also been expressed with replication-competent vectors to improve cell killing.[26–30] One important factor to keep in mind is to enhance antitumor effect without inhibiting the proliferative capacity of viruses.

In summary, oncolytic adenovirotherapy in combination with Bax gene therapy resulted in augmented cell killing *in vitro*. However, in a xenografted tumor model, oncolytic efficacy was not improved; this was associated with suppressed E1A protein expression and reduced viral replication. Bax gene therapy may possibly interfere with viral production and thus be not conducive to oncolytic virotherapy.

Acknowledgements

This work was supported in part by grants from the Ministry of Education, Culture, Sports, Science and Technology of Japan (T.F. and S.K.); and by grants from the Ministry of Health, Labour and Welfare of Japan (T.F. and S.K.).

References

1. Hawkins LK, Lemoine NR, Kirn D. Oncolytic biotherapy: a novel therapeutic platform. Lancet Oncol 2002;3:17–26.
2. Chiocca EA. Oncolytic viruses. Nat Rev Cancer 2002;2:938–50.
3. Nemunaitis J, Khuri F, Ganly I, Arseneau J, Posner M, Vokes EK, McCarty T, Landers S, Blackburn A, Romel L, Randlev B, Kaye S, et al. Phase II trial of intratumoral administration of ONYX-015, a replication-selective adenovirus, in patients with refractory head and neck cancer. J Clin Oncol 2001;19:289–98.
4. Khuri FR, Nemunaitis J, Ganly I, Arseneau J, Tannock IF, Romel L, Gore M, Ironside J, MacDougall RH, Heise C, Randlev B, Gillenwater AM, et al. A controlled trial of intratumoral ONYX-015, a selectively-replicating adenovirus, in combination with cisplatin and 5-fluorouracil in patients with recurrent head and neck cancer. Nat Med 2000;6:879–85.
5. Harrison D, Sauthoff H, Heitner S, Jagirdar J, Rom W, Hay J. Wild-type adenovirus decreases tumor xenograft growth, but despite viral persistence complete tumor responses are rarely achieved-deletion of the viral E1b-19kDa gene increases the oncolytic effect. Hum Gene Ther 2001;12:1323–32.
6. DeWeese TL, van der Poel H, Li S, Mikhak B, Drew R, Goemann M, Hamper U, DeJong R, Detorie N, Rodriguez R, Haulk T, DeMarzo AM, et al. A phase I trial of CV706, a replication-competent, PSA selective oncolytic adenovirus, for the treatment of locally recurrent prostate cancer following radiation therapy. Cancer Res 2001;61:7464–72.
7. Reid T, Galanis E, Abbruzzese J, Sze D, Wein LM, Andrews J, Randlev B, Heise C, Uprichard M, Hatfield M, Rome L, Rubin J, et al. Hepatic arterial infusion of a replication-selective oncolytic adenovirus (dl1520): phase II viral, immunologic, and clinical endpoints. Cancer Res 2002;62:6070–79.
8. Hamid O, Varterasian ML, Wadler S, Hecht JR, Benson A, Galanis E, Uprichard M, Omer C, Bycott P, Hackman RC, Shields AF. Phase II trial of intravenous CI-1042 in patients with metastatic colorectal cancer. J Clin Oncol 2003;21:1498–504.
9. Jurgensmeier JM, Xie Z, Deveraux Q, Ellerby L, Bredesen D, Reed JC. Bax directly induces release of cytochrome c from isolated mitochondria. Proc Natl Acad Sci USA 1998;95:4997–5002.
10. Pastorino JG, Chen ST, Tafani M, Snyder JW, Farber JL. The overexpression of Bax produces cell death upon induction of the mitochondrial permeability transition. J Biol Chem 1998;273:7770–5.
11. Kagawa S, Pearson SA, Ji L, Xu K, McDonnell TJ, Swisher SG, Roth JA, Fang B. A binary adenoviral vector for expressing high levels of the proapoptotic gene bax. Gene Ther 2000;7:75–9.
12. Kagawa S, Gu J, Swisher SG, Ji L, Roth JA, Lai D, Stephens LC, Fang B. Antitumor effect of adenovirus-mediated Bax gene transfer on p53-sensitive and p53-resistant cancer lines. Cancer Res 2000;60:1157–61.
13. Tsunemitsu Y, Kagawa S, Tokunaga N, Otani S, Umeoka T, Roth JA, Fang B, Tanaka N, Fujiwara T. Molecular therapy for peritoneal dissemination of xenotransplanted human MKN-45 gastric cancer cells with adenovirus mediated Bax gene transfer. Gut 2004;53:554–60.
14. Kawashima T, Kagawa S, Kobayashi N, Shirakiya Y, Umeoka T, Teraishi F, Taki M, Kyo S, Tanaka N, Fujiwara T. Telomerase-specific replication-selective virotherapy for human cancer. Clin Cancer Res 2004;10:285–92.
15. Maizel JV, Jr, White DO, Scharff MD. The polypeptides of adenovirus. I. Evidence for multiple protein components in the virion and a comparison of types 2, 7A, and 12. Virology 1968;36:115–25.
16. Kanegae Y, Makimura M, Saito I. A simple and efficient method for purification of infectious recombinant adenovirus. Jpn J Med Sci Biol 1994;47:157–66.
17. Sauthoff H, Heitner S, Rom WN, Hay JG. Deletion of the adenoviral E1b-19kD gene enhances tumor cell killing of a replicating adenoviral vector. Hum Gene Ther 2000;11:379–88.
18. Chiou SK, White E. Inhibition of ICE-like proteases inhibits apoptosis and increases virus production during adenovirus infection. Virology 1998;244:108–18.
19. Lambright ES, Amin K, Wiewrodt R, Force SD, Lanuti M, Propert KJ, Litzky L, Kaiser LR, Albelda SM. Inclusion of the herpes simplex thymidine kinase gene in a replicating adenovirus does not augment antitumor efficacy. Gene Ther 2001;8:946–53.
20. Liu TC, Hallden G, Wang Y, Brooks G, Francis J, Lemoine N, Kirn D. An E1B-19kDa gene deletion mutant adenovirus demonstrates tumor necrosis factor-enhanced cancer selectivity and enhanced oncolytic potency. Mol Ther 2004;9:786–803.
21. Kim J, Cho JY, Kim JH, Jung KC, Yun CO. Evaluation of E1B gene-attenuated replicating adenoviruses for cancer gene therapy. Cancer Gene Ther 2002;9:725–36.
22. Doronin K, Toth K, Kuppuswamy M, Ward P, Tollefson AE, Wold WS. Tumor-specific, replication-competent adenovirus vectors overexpressing the adenovirus death protein. J Virol 2000;74:6147–55.
23. Sova P, Ren XW, Ni S, Bernt KM, Mi J, Kiviat N, Lieber A. A tumor-targeted and conditionally replicating oncolytic adenovirus vector expressing TRAIL for treatment of liver metastases. Mol Ther 2004;9:496–509.
24. Liu XY, Qiu SB, Zou WG, Pei ZF, Gu JF, Luo CX, Ruan HM, Chen Y, Qi YP, Qian C. Effective gene—virotherapy for complete eradication of tumor mediated by the combination of hTRAIL (TNFSF10) and plasminogen k5. Mol Ther 2005;11:531–41.
25. Ye X, Lu Q, Zhao Y, Ren Z, Ren XW, Qiu QH, Tong Y, Liang M, Hu F, Chen HZ. Conditionally replicative adenovirus vector carrying TRAIL gene for enhanced oncolysis of human hepatocellular carcinoma. Int J Mol Med 2005;16:1179–84.
26. Bristol JA, Zhu M, Ji H, Mina M, Xie Y, Clarke L, Forry-Schaudies S, Ennist DL. In vitro and in vivo activities of an oncolytic adenoviral vector designed to express GM-CSF. Mol Ther 2003;7:755–64.
27. Ramesh N, Ge Y, Ennist DL, Zhu M, Mina M, Ganesh S, Reddy PS, Yu DC. CG0070, a conditionally replicating granulocyte macrophage colony-stimulating factor—armed oncolytic adenovirus for the treatment of bladder cancer. Clin Cancer Res 2006;12:305–13.
28. Zhao L, Gu J, Dong A, Zhang Y, Zhong L, He L, Wang Y, Zhang J, Zhang Z, Huiwang J, Qian Q, Qian C, et al. Potent antitumor activity of oncolytic adenovirus expressing mda-7/IL-24 for colorectal cancer. Hum Gene Ther 2005;16:845–58.
29. Nanda D, Vogels R Havenga M, Avezaat CJ, Bout A, Smitt PS. Treatment of malignant gliomas with a replicating adenoviral vector expressing herpes simplex virus-thymidine kinase. Cancer Res 2001;61:8743–50.
30. Lee CT, Park KH, Yanagisawa K, Adachi Y, Ohm JE, Nadaf S, Dikov MM, Curiel DT, Carbone DP. Combination therapy with conditionally replicating adenovirus and replication defective adenovirus. Cancer Res 2004;64:6660–5.

Gene Therapy (2008) 15, 1233–1239

www.nature.com/gt

SHORT COMMUNICATION

Autophagy-inducing agents augment the antitumor effect of telomerase-selective oncolytic adenovirus OBP-405 on glioblastoma cells

T Yokoyama[1,8], E Iwado[1,8], Y Kondo[1], H Aoki[1], Y Hayashi[2], MM Georgescu[2], R Sawaya[1,3], KR Hess[4], GB Mills[5], H Kawamura[6], Y Hashimoto[6], Y Urata[6], T Fujiwara[6,7] and S Kondo[1,3]

[1]*Department of Neurosurgery, The University of Texas MD Anderson Cancer Center, Houston, TX, USA;* [2]*Department of Neuro-Oncology, The University of Texas MD Anderson Cancer Center, Houston, TX, USA;* [3]*Department of Neurosurgery, Baylor College of Medicine, Houston, TX, USA;* [4]*Department of Biostatistics and Applied Mathematics, The University of Texas MD Anderson Cancer Center, Houston, TX, USA;* [5]*Department of Molecular Therapeutics, The University of Texas MD Anderson Cancer Center, Houston, TX, USA;* [6]*Oncolys BioPharma Inc., Tokyo, Japan and* [7]*Division of Surgical Oncology, Department of Surgery, Okayama University Graduate School of Medicine and Dentistry, Okayama, Japan*

Oncolytic adenoviruses are a promising tool in cancer therapy. In this study, we characterized the role of autophagy in oncolytic adenovirus-induced therapeutic effects. OBP-405, an oncolytic adenovirus regulated by the human telomerase reverse transcriptase promoter (hTERT-Ad, OBP-301) with a tropism modification (RGD) exhibited a strong antitumor effect on glioblastoma cells. When autophagy was inhibited pharmacologically, the cytotoxicity of OBP-405 was attenuated. In addition, autophagy-deficient Atg5$^{-/-}$ *mouse embryonic fibroblasts (MEFs) were less sensitive than wild-type MEFs to OBP-405. These findings indicate that OBP-405-induced autophagy is a cell killing effect. Moreover, autophagy-inducing therapies (temozolomide and rapamycin) synergistically sensitized tumor cells to OBP-405 by stimulating the autophagic pathway without altering OBP-405 replication. Mice harboring intracranial tumors treated with OBP-405 and temozolomide survived significantly longer than those treated with temozolomide alone, and mice treated with OBP-405 and the rapamycin analog RAD001 survived significantly longer than those treated with RAD001 alone. The observation that autophagy inducers increase OBP-405 antitumor activity suggests a novel strategy for treating patients with glioblastoma.*
Gene Therapy (2008) **15,** 1233–1239; doi:10.1038/gt.2008.98; published online 26 June 2008

Keywords: *autophagy; glioblastoma; OBP-301; OBP-405*

Oncolytic adenoviruses have recently been developed as a novel cancer therapy.[1,2] We have shown that the oncolytic adenovirus regulated by the human telomerase reverse transcriptase promoter (hTERT-Ad) induces nonapoptotic autophagy in glioblastoma cells.[3] However, the molecular machinery underlying autophagy-induced cell death remains unclear.[4–6] Furthermore, the processes determining whether autophagy in cancer cells causes death or acts as a protective mechanism activated during cellular distress are unknown. In this study, we elucidated the therapeutic role of autophagy in hTERT-Ad infection.

The infection efficiency of adenoviral constructs, which are derived from human adenovirus serotype 5, varies widely depending on the cellular expression of the coxsackievirus and adenovirus receptor (CAR).[7] Modification of the adenoviral fiber protein is one approach to overcoming the limitation imposed by this dependence on CAR.[8] A recent study demonstrated the activity of OBP-405, which is an hTERT-Ad with a tropism modification (RGD): OBP-405 had a profound oncolytic effect *in vitro* and *in vivo* on lung and colon cancer cells regardless of the CAR expression level.[9] In addition, for cells with low CAR expression levels, OBP-405 had a higher rate of infection than did OBP-301, an hTERT-Ad that expresses the *E1A* gene under the control of a 455-bp hTERT promoter.[9] The hTERT-Ad that we used previously has a 255-bp hTERT promoter.[3]

Good manufacturing practice OBP-301 (Telomelysin) and OBP-405 (Telomelysin-RGD) were used in the current study. We first determined the expression levels of CAR and integrins (αvβ3 and αvβ5) on the cell surface of glioblastoma cells. To predict the response of human glioblastoma to OBP-301 or OBP-405, the established cell lines U87-MG, U251-MG, D54, and U373-MG and primary MDC-01 cells isolated from glioblastoma tissue were used. The U87-MG, D54 and MDC-01 cells expressed the lowest levels of CAR, whereas the U251-MG cells expressed the highest level of CAR (Figure 1a). In contrast, αvβ3 and αvβ5 integrins were highly expressed in each of these glioblastoma cells. Cells that expressed low levels of CAR were resistant to OBP-301 infection, whereas OBP-405 effectively decreased viabi-

Correspondence: Dr T Yokoyama, Department of Neurosurgery, The University of Texas MD Anderson Cancer Center, Unit BSRB 1004, 1515 Holcombe Blvd., Houston, TX 77030, USA.
E-mail: tyokoyama@mdanderson.org
[8]These authors contributed equally to this work.
Received 26 January 2008; revised 1 April 2008; accepted 1 April 2008; published online 26 June 2008

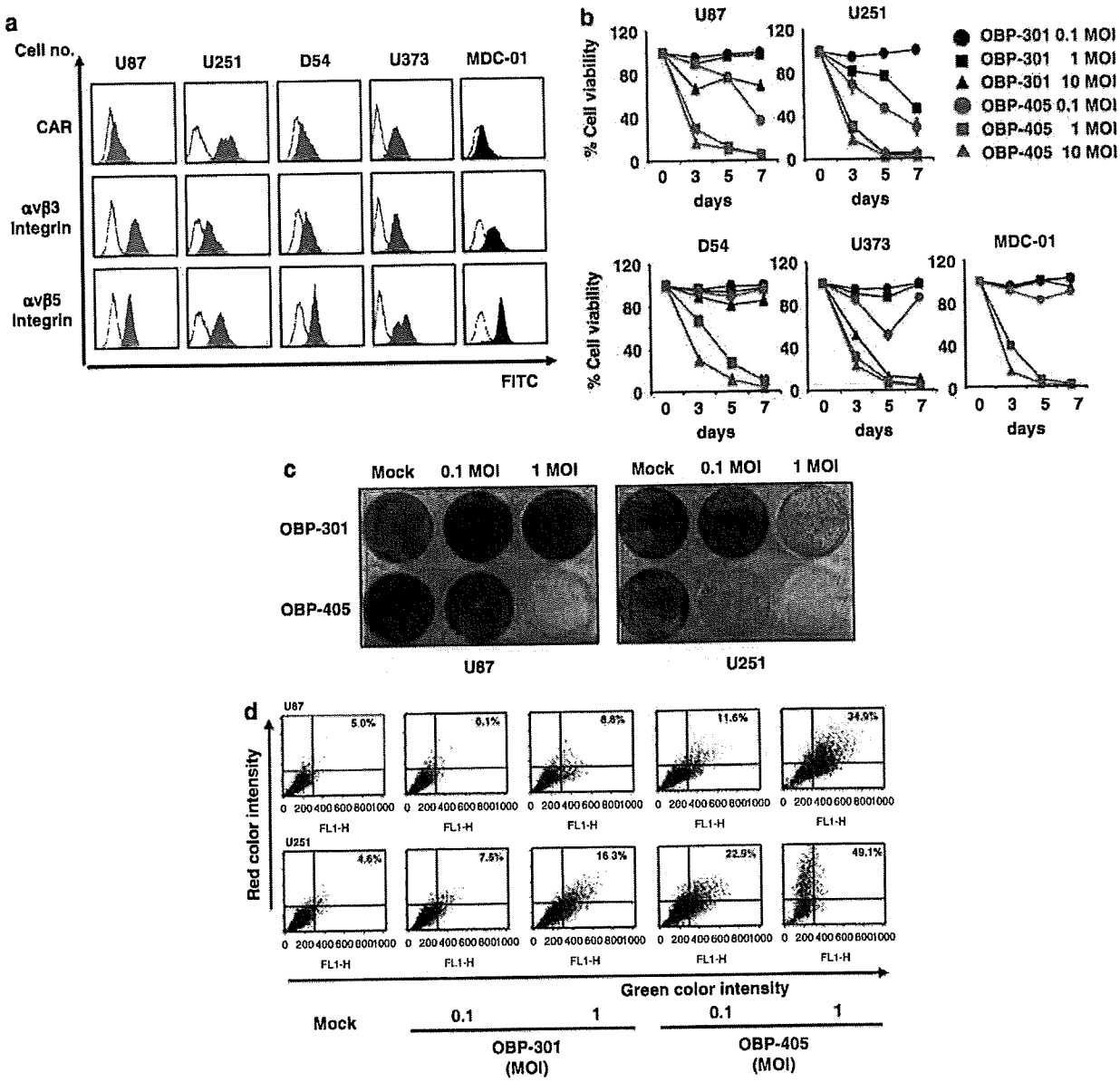

Figure 1 (a) Flow cytometric analysis of CAR and integrin (αvβ3 and αvβ5) expression on glioblastoma cells. Human glioblastoma cell lines U87-MG, U251-MG, D54 and U373-MG were purchased from American Type Culture Collection (Manassas, VA, USA). Primary glioblastoma MDC-01 cells were isolated from surgical specimens of glioblastoma at MD Anderson Cancer Center and were positive for telomerase and anti-glial-fibrillary acidic protein. Cells were incubated with anti-CAR (Upstate Biotechnology, Lake Placid, NY, USA), anti-αvβ3 integrin and anti-á$_v$β5 integrin (Chemicon International, Temecula, CA, USA) monoclonal antibodies and then detected with fluorescein isothiocyanate (FITC)-labeled rabbit anti-mouse IgG secondary antibody (Zymed Laboratories, San Francisco, CA, USA). Open areas (control), isotype-matched normal mouse IgG1 conjugated to FITC. (b) Effect of OBP-301 and OBP-405 on the viability of glioblastoma cells. Cells were infected at the indicated MOI values and surviving cells were quantified over 7 days by the use of WST-1 assay (Roche Applied Science, Indianapolis, IN, USA). Results shown are the means ± s.d. of three independent experiments. (c) Oncolytic effect of OBP-301 and OBP-405 on glioblastoma cells. Low-CAR expressing (U87-MG) and high-CAR expressing (U251-MG) cells were stained with 0.5% crystal violet (Sigma-Aldrich, St Louis, MO, USA) 5 days after infection. (d) Development of acidic vesicular organelles (AVOs) in U87-MG and U251-MG cells infected with OBP-301 or OBP-405 at an MOI of 0.1 or 1.0 for 72 h. Mock- or virus-infected cells were stained with 1.0 μg ml^{-1} acridine orange (Polysciences, Warrington, PA, USA) for 15 min at room temperature and analyzed using a flow cytometer (FACScan; Becton Dickinson, San Jose, CA, USA). In acridine orange-stained cells, the cytoplasm and nucleus fluorescence bright green and dim red, whereas acidic compartments fluorescence bright red.[10,11] The intensity of the red fluorescence is proportional to the degree of acidity and volume of AVOs. Top of grid was considered as AVOs. CAR, coxsackievirus and adenovirus receptor; IgG, immunoglobulin G; MOI, multiplicity of infection.

lity of glioblastoma cells (Figure 1b). In addition, OBP-405 killed the cells more efficiently than did OBP-301, and neither OBP-301 nor OBP-405 induced apoptosis (Figure 1c) (Supplementary Figures 1a–c).

Nonapoptotic autophagy is characterized by the development of acidic vesicular organelles (AVOs).[10] Compared with mock infection, both OBP-301 and OBP-405 increased the percentage of AVO-positive cells in a multiplicity of infection (MOI)-dependent manner (Figure 1d). As expected, OBP-405 induced the development of AVOs more efficiently than did OBP-301.

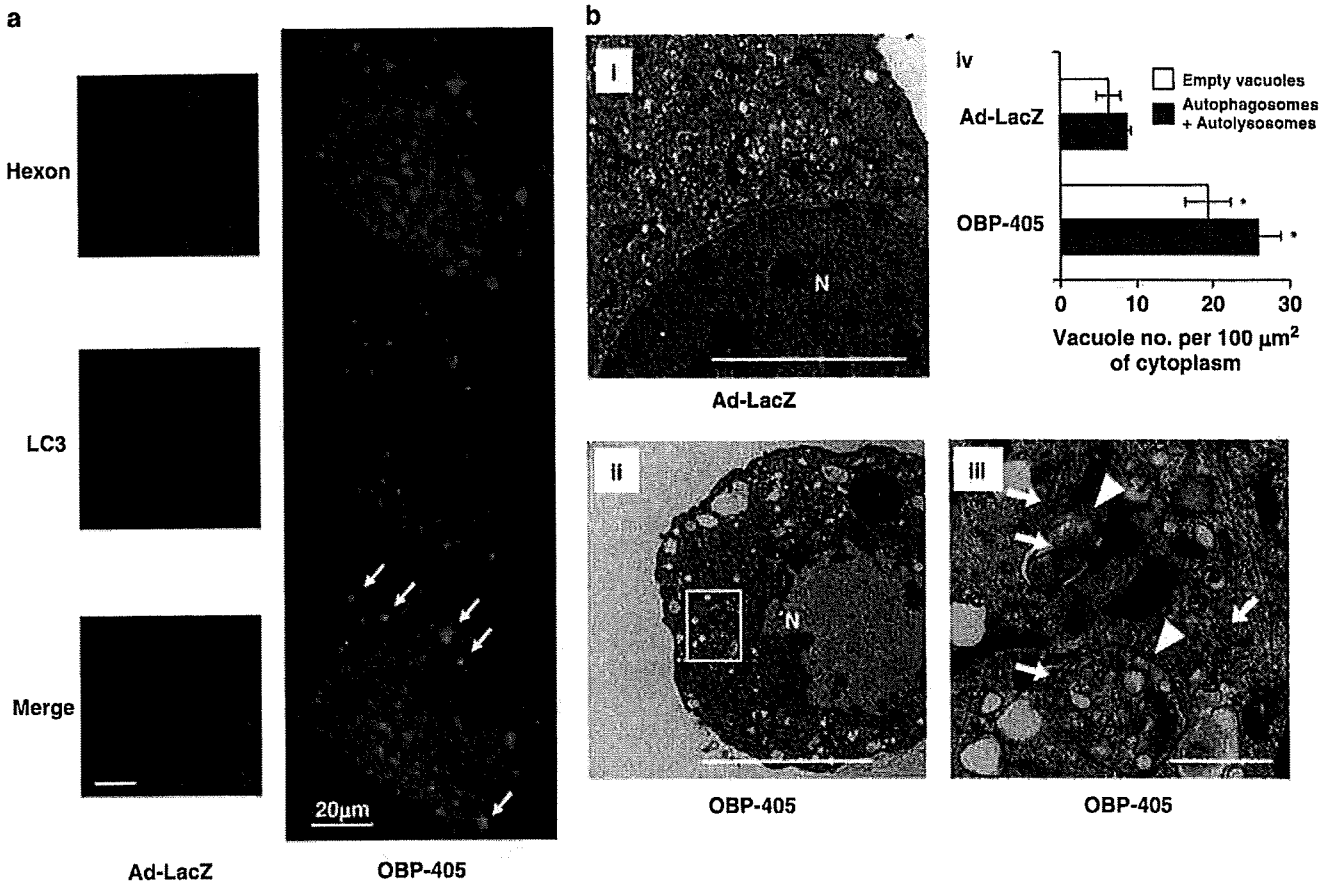

Figure 2 (a) Localization of the adenoviral protein hexon and autophagic LC3B protein in glioblastoma cells infected with Ad-LacZ or OBP-405 at an MOI of 0.5. After infection for 72 h, U87-MG cells were processed for fluorescent immunocytostaining with anti-LC3B (1:5000 dilution) and antiadenovirus 1, 2, 5 and 6 hexon (Chemicon International) antibodies. Anti-LC3B antibody was generated as described previously.[14,15] The slides were monitored using inverted microscope (ECRIPSE TE2000-U; Nikon, Melville, NY, USA) and the data were deconvolved and analyzed using AutoQuant's AutoDeBlur software (MediaCybernetics, Bethesda, MD, USA). The arrow shows the colocalization of LC3B and hexon. (b) Electron photomicrographs showing the ultrastructure, including the nucleus (N) of glioblastoma cells treated with nonreplicating adenovirus carrying the Ad-LacZ or OBP-405 at an MOI of 0.5 for 72 h. (i) Ad-LacZ-infected U87-MG cells; few autophagic vacuoles were observed, scale bar = 10 μm. (ii) OBP-405-infected U87-MG cells, scale bar = 10 μm. (iii) A magnified view of the area boxed in (ii), scale bar = 1 μm. The arrow indicates viral particles and the arrowhead indicates an autophagosome that includes residual material and virus particles in the cytoplasm. (iv) Autophagosomes and autolysosomes were quantified, as described previously.[16,17] $^*P<0.05$ vs Ad-LacZ. MOI, multiplicity of infection.

The green fluorescent protein (GFP)-tagged expression vector of LC3 is a useful tool with which to detect autophagy.[12] On fluorescence microscopy, GFP-LC3-transfected U87-MG cells showed the diffuse distribution of GFP-LC3 with mock infection, whereas infection with OBP-405 at an MOI of 1.0 resulted in a punctate pattern of GFP–LC3 (Supplementary Figure 2a). This pattern represents autophagic vacuoles and indicated that OBP-405 induced autophagy. With both OBP-301 and OBP-405, the percentage of GFP–LC3 dots increased in an MOI-dependent manner; this increase was considerably higher with OBP-405 than with OBP-301.

The LC3 protein exists in two cellular forms, LC3-I and LC3-II. LC3-I is converted to LC3-II by conjugation to phosphatidylethanolamine, and the amount of LC3-II is closely correlated with the number of autophagosomes.[13] In both U87-MG and U251-MG cells, the amount of LC3-II was increased by infection with OBP-301 or OBP-405 in an MOI-dependent manner and by OBP-405 in a time-dependent manner (Supplementary Figure 2b). These results indicated that OBP-405 caused more autophagy in glioblastoma cells than OBP-301 did.

To analyze the association between adenoviral infection and autophagy, we determined the localization of OBP-405 and autophagic vacuoles. The adenoviral hexon was detected in the cytoplasm 6 h after infection, but at that point, autophagic vacuoles positive for the isoform B of human LC3 (LC3B) were not observed (Supplementary Figure 3), indicating that autophagy was not initiated. Twenty-four hours after infection, hexon was detected in the cytoplasm and nucleus and LC3B-positive autophagic vacuoles were observed. At 48 h, the cell and nucleus had become larger. At 72 h after infection, the majority of the autophagic vacuoles were colocalized with hexon-positive adenoviruses (Figure 2a). In addition, we analyzed the ultrastructure of infected U87-MG cells. U87-MG cells infected with control nonreplicating adenovirus (Ad-LacZ) exhibited few autophagic features, whereas autophagic vacuoles, autolysosomes and empty vacuoles were observed after infection with OBP-405. Most OBP-405-infected cells

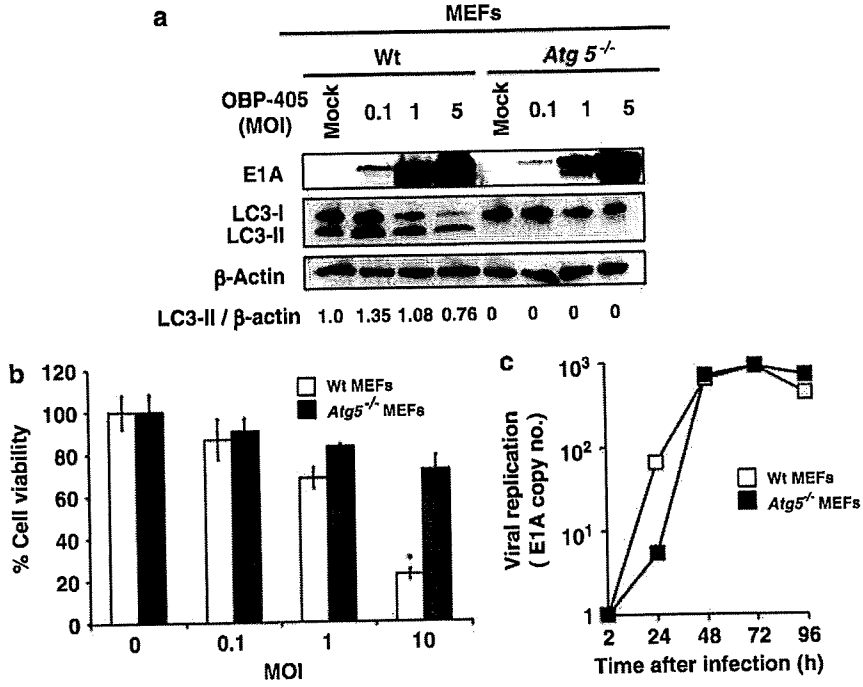

Figure 3 (a) Effect of OBP-405 infection on the wild-type and *Atg5*$^{-/-}$ MEFs (kindly provided by Dr N Mizushima). The expression of E1A (BD Biosciences Pharmingen, San Diego, CA, USA) and an amount of LC3-II in MEFs infected with OBP-405 at an MOI of 0–5.0 for 72 h was assessed by western blotting. The intensities of the amount of LC3-II bands were normalized by the bands' intensities of β-actin (Sigma-Aldrich), using Bio-Rad Fluor-S Multiimager (Bio-Rad Laboratories, Hercules, CA, USA). (b) Effect of OBP-405 on the viability of wild-type and *Atg5*$^{-/-}$ MEFs. MEFs were infected with OBP-405 at an MOI of 0 to 10 for 48 h, and cell viability was assessed by WST-1 assay. *$P<0.01$ vs *Atg5*$^{-/-}$ MEFs. (c) E1A viral replication of wild-type and *Atg5*$^{-/-}$ MEFs infected with OBP-405 at an MOI of 1.0. The cells were incubated at 37 °C for the indicated periods, trypsinized and harvested for intracellular replication analysis at 2, 24, 48, 72 and 96 h. DNA purification was performed with the QIAmp DNA mini kit (Qiagen, Valencia, CA, USA). The E1A DNA copy number was determined by quantitative real-time PCR, using a Power SYBR Green PCR Master Mix (Applied Biosystems, Foster, CA, USA) and 7500 real-time PCR systems (Applied Biosystems), as described previously.[9] The amount of viral E1A copy number is defined as the fold increase for each sample relative to that at 2 h. MEFs, mouse embryonic fibroblasts; MOI, multiplicity of infection

exhibited viral particles in the nucleus and cytoplasm, but they exhibited neither the chromatin condensation nor the DNA fragmentation that is the characteristic of apoptosis (Figure 2b). Interestingly, viral particles were observed inside autophagic vacuoles. These results suggested that OBP-405 infection initiated the autophagic process and that the autophagic vacuoles sequestered replicating OBP-405.

To assess the role of autophagy in OBP-405 infection, we inhibited the OBP-405-induced autophagy pharmacologically by using 3-methyladenine (3-MA);[18] the decreased viability of these cells was significantly reversed ($P<0.01$) (Supplementary Figures 4a and b). However, the inhibition of autophagy did not affect the increase in E1A copy number of OBP-405 (Supplementary Figure 4c). To exclude the possibility that the effects of 3-MA are independent of inhibition of autophagy, we inhibited autophagy specifically by using small interfering RNA (siRNA) directed against *autophagy-related gene 5* (*Atg5*), which is essential for autophagosome formation. Transfection with *Atg5* siRNA effectively inhibited OBP-405-induced autophagy and recovered the OBP-405-inhibited viability of U87-MG and U251-MG cells (Supplementary Figure 5a–c). Together, the results indicated that OBP-405 induced cell death through autophagy.

In addition, *Atg5*$^{-/-}$ mouse embryonic fibroblasts (MEFs) were significantly more resistant to OBP-405-induced death than the wild-type MEFs ($P<0.01$) (Figures 3a and b). This observation supported our results with 3-MA and *Atg5* siRNA. Similar to 3-MA, viral replication of OBP-405 did not differ significantly between the wild-type and *Atg5*$^{-/-}$ MEFs (Figure 3c).

The above observations prompted us to hypothesize that the antitumor effect of OBP-405 would be augmented by the combinatorial therapy with other autophagy-inducing agents. To test our hypothesis, we combined OBP-405 with rapamycin, an inhibitor of the mammalian target of rapamycin and the DNA-alkylating agent temozolomide (TMZ), both of which efficiently induce autophagy.[19,20] Rapamycin and TMZ not only enhanced OBP-405-induced autophagy *in vitro* but also synergized with OBP-405 to induce the death of glioblastoma cells (Figures 4a and b; Supplementary Figure 6). In contrast, TMZ or rapamycin did not alter viral replication (Figure 4c). Thus OBP-405 synergizes with autophagy-inducing agents to increase cell death *in vitro*.

To determine whether the *in vitro* effect of OBP-405 with TMZ or rapamycin translates to greater activity *in vivo*, we established intracranial tumors in nude mice. Compared with mice treated with Ad-LacZ, mice treated with OBP-405 lived significantly longer (mean survival = 27.5 vs 34.0 days; difference (95% confidence interval) = 6.0 (3.0–9.1) days; $P=0.0008$) (Figure 5a). Mice treated with TMZ also survived significantly longer (mean survival = 27.5 vs 37.0 days; difference = 10

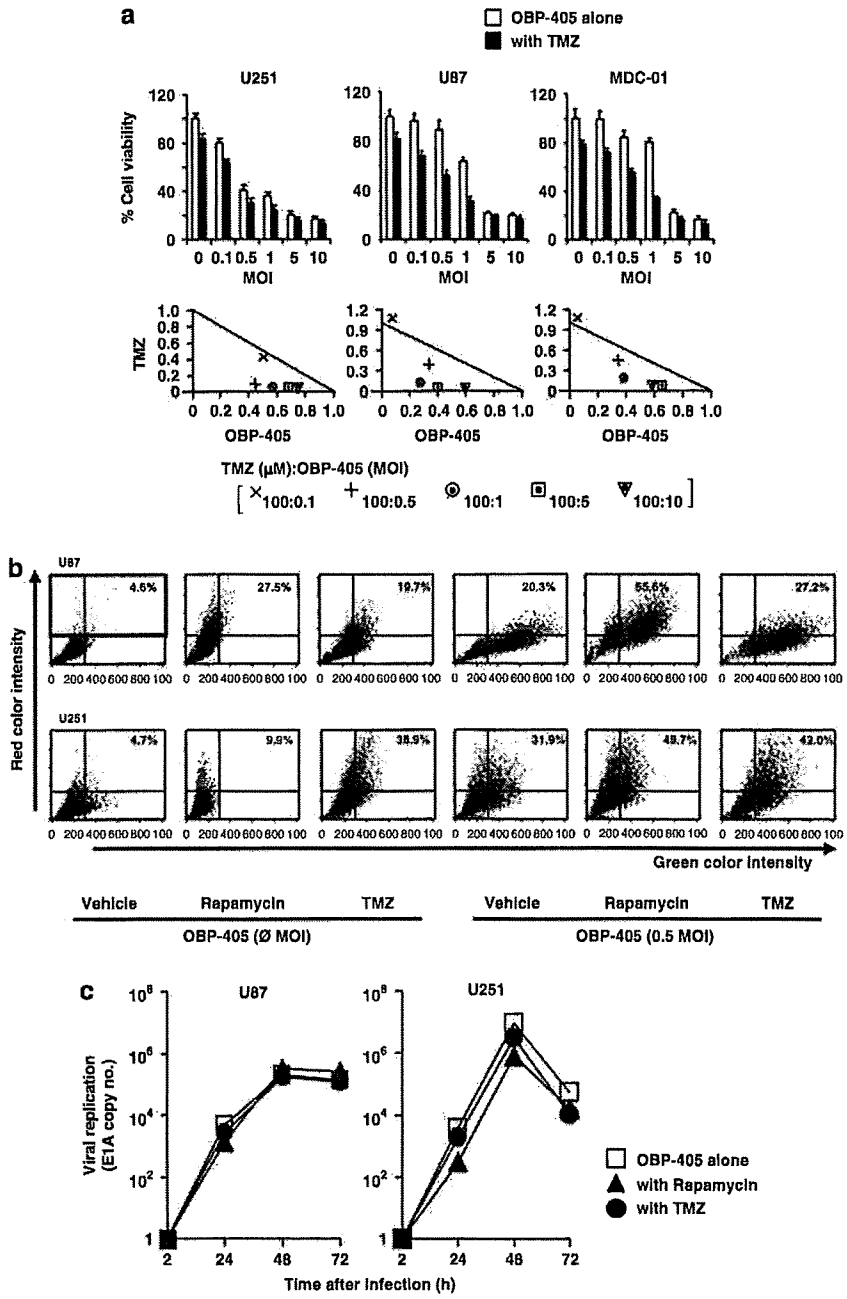

Figure 4 (a) Combined effects of OBP-405 with TMZ on glioblastoma cells. U251-MG, U87-MG and MDC-01 cells were infected with OBP-405 at an MOI of 0 to 10 in the presence of 100 μM TMZ (purchased from a pharmacy in The University of Texas MD Anderson Cancer Center) for 72 h for the WST-1 assay. The combined effect of OBP-405 with TMZ was analyzed with the combination index (CI)-isobologram using CalcuSyn software (Biosoft, Ferguson, MO, USA), as described previously.[19] In the isobologram, a plot on the diagonal line indicates that the combination is simply additive. A plot to the left under the line indicates that the combination is synergistic, whereas a plot to the right above the line indicates that it is antagonistic. Each plot represents values generated in at least three independent experiments for the simultaneous treatment of cells. (b) Development of acidic vesicular organelles (AVOs) in U87-MG and U251-MG cells infected with OBP-405 at an MOI of 0.5 in the presence of 1 nM rapamycin (Sigma-Aldrich) or 100 μM TMZ were stained with 1.0 μg ml^{-1} acridine orange as described previously.[10,11] Top of grid was considered as AVOs. (c) E1A viral replication of U87-MG and U251-MG cells infected with OBP-405 at an MOI of 0.5 alone or with 1 nM rapamycin or 100 μM TMZ over 72 h as described previously.[9] MOI, multiplicity of infection; TMZ, temozolomide.

(7.0–12) days; $P<0.001$), but RAD001-treated mice did not (mean survival = 27.5 vs 30.5 days; difference = 4 (−1 to 9) days; $P=0.14$). Strikingly, mice treated with OBP-405 and TMZ survived significantly longer than those treated with TMZ alone (mean = 53.0 vs 37.0 days; difference = 15.1 (7.2–23.1) days; $P=0.0015$), and mice treated with OBP-405 and RAD001 survived significantly longer than those treated with RAD001 alone (mean = 38.0 vs 30.5 days; difference = 9.3 (1.7–16.8) days, $P=0.021$). Finally, compared with results using OBP-405 alone, the survival time of mice was significantly prolonged by combination with TMZ (difference = 19 (11–26) days, $P=0.0001$) or RAD001 (difference = 7 (1–13) days, $P=0.025$).

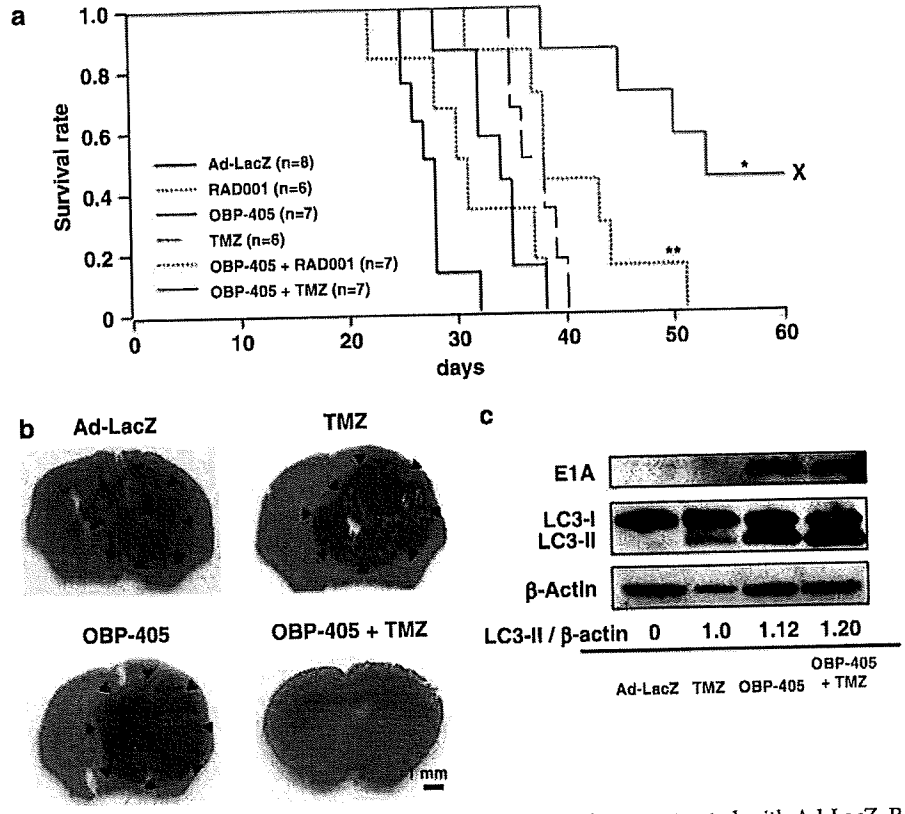

Figure 5 (a) Curves showing overall survival of mice bearing U87-MG intracranial tumors treated with Ad-LacZ, RAD001, TMZ, OBP-405, OBP-405 plus RAD001 or OBP-405 plus TMZ. The Kaplan–Meier method and pooled-variance two-tailed t-test were used to assess the statistical significance of differences in survival time; $^{*}P = 0.0015$ vs TMZ; $^{**}P = 0.021$ vs RAD001; 8- to 12-week-old female nude mice (Department of Experimental Radiation Oncology, MD Anderson Cancer Center) were used. The intracranial tumor model using U87-MG cells (5×10^5) was established as described previously.[3] Three days after the inoculation of U87-MG cells (day 0), the treatments were initiated as follows. On days 3, 5 and 7, through a 10 μl Hamilton syringe fitted with a 26-gauge needle connected to a microinfusion pump, Ad-LacZ (2.2×10^9 pfu ml^{-1}) or OBP-405 (2.2×10^9 pfu ml^{-1}) in 10 μl of sterile PBS was infused into the tumors through the screw guide at a depth of 3.5 mm from the skull. Two hundred microliters of TMZ (7.5 mg kg^{-1} in PBS with 5% dimethyl sulfoxide) was injected intraperitoneally five times a week for 2 weeks, and RAD001 (5 mg kg^{-1} in water, kindly supplied by Norvartis, Basel, Switzerland) was administered orally every day until the animals became moribund and were killed. (b) Hematoxylin and eosin-stained brain tissues of mice bearing intracranial U87-MG tumors treated with Ad-LacZ (day 32), TMZ (day 40), OBP-405 (day 38) or OBP-405 plus TMZ (day 60). Scale bar = 1 mm. (c) Western blots showing induction of autophagy and expression of E1A in intracerebral tumors treated with Ad-LacZ (day 28), TMZ (day 39), OBP-405 (day 35) or OBP-405 plus TMZ (day 53). Anti-LC3B antibody and anti-E1A antibody were used. The intensities of the amount of LC3-II bands were normalized by the bands' intensities of β-actin. PBS, phosphate-buffered saline; TMZ, temozolomide.

The intracranial tumors of mice treated with Ad-LacZ, OBP-405, TMZ or RAD001 alone grew extensively, with midlines shifted laterally. Strikingly, tumors were undetectable in brain tissue harvested from three mice treated with OBP-405 plus TMZ that survived 60 days after inoculation (Figure 5b). Hexon was detected in the intracranial tumor treated with OBP-405 plus TMZ (day 45) but not in the tumor treated with Ad-LacZ (day 28) (Supplementary Figure 7). This finding was supported by western blotting results showing detectable E1A protein expression in intracranial tumors treated with OBP-405 alone or with TMZ (Figure 5c). These results indicated that OBP-405 replicated and spread through the intracranial tumors but not through the normal brain tissues and supported the contention that the effect of OBP-405 is specific to tumors, likely due to the hTERT promoter activity. Then, we determined whether the induction of autophagy is detected under *in vivo* settings using an anti-LC3B-specific antibody. As shown in Figure 5c, the amount of LC3-II was higher in intracranial tumors of mice treated with TMZ, OBP-405 and OBP-405 plus TMZ than in Ad-LacZ-treated mice. These results indicated that autophagy was induced in intracranial tumors of mice as well as *in vitro* and that the extent of autophagy was enhanced by the combination treatment. However, intracranial tumors established from noninvasive glioblastoma cell lines may limit the clinical relevance of studies assessing the efficacy of novel therapies.[21] Therefore, we will further assess whether the treatment with OBP-405 plus TMZ or RAD001 prolong the survival of the mice carrying invasive intracranial tumors.[21]

In conclusion, we found that the fiber-modified hTERT-Ad OBP-405 has a marked antitumor effect on glioblastoma cells regardless of the cellular expression level of CAR. Moreover, autophagy-inducing agents (TMZ and rapamycin) increase the *in vitro* and *in vivo* antitumor activity of OBP-405 through the enhancement of autophagic pathway. A recent clinical study showed that TMZ had antitumor activity both as a single agent

and as adjuvant chemotherapy for patients with malignant gliomas, although its efficacy was modest.[22] Our study results might indicate a new way to treat glioblastomas with a combination of autophagy-inducing agents.

Acknowledgements

We thank Dr Noboru Mizushima for the GFP-LC3 expression vector and the wild-type and *Atg5−/−* MEFs. We also thank E Faith Hollingsworth for technical support and Elizabeth L Hess for editing the manuscript. This work was supported in part by Grant CA-088936 from the National Cancer Institute (to S Kondo), by a generous donation from the Anthony D Bullock III Foundation (to Y Kondo, R Sawaya and S Kondo) and the Institutional Core Grant CA-16672 High Resolution Electron Microscopy Facility, MD Anderson Cancer Center.

Grant support: This study was supported in part by National Cancer Institute Grants CA088936 and CA108558, a start-up fund from The University of Texas MD Anderson Cancer Center (SK), a generous donation from the Anthony D Bullock III Foundation (YK, RS and SK) and the cancer center support grant (CCSG)/shared resources of MD Anderson Cancer Center.

References

1 Mathis JM, Stoff-Khalili MA, Curiel DT. Oncolytic adenoviruses-selective retargeting to tumor cells. *Oncogene* 2005; **24**: 7775–7791.
2 Ko D, Hawkins L, Yu DC. Development of transcriptionally regulated oncolytic adenoviruses. *Oncogene* 2005; **24**: 7763–7774.
3 Ito H, Aoki H, Kühnel F, Kondo Y, Kubicka S, Wirth T *et al*. Autophagic cell death of malignant glioma cells induced by a conditionally replicating adenovirus. *J Natl Cancer Inst* 2006; **98**: 625–636.
4 Ogier-Denis E, Codogno P. Autophagy: a barrier or an adaptive response to cancer. *Biochim Biophys Acta* 2003; **1603**: 113–128.
5 Gozuacik D, Kimchi A. Autophagy as a cell death and tumor suppressor mechanism. *Oncogene* 2004; **23**: 2891–2906.
6 Kondo Y, Kanzawa T, Sawaya R, Kondo S. The role of autophagy in cancer development and response to therapy. *Nat Rev Cancer* 2005; **5**: 726–734.
7 Wickham TJ, Mathias P, Cheresh DA, Nemerow GR. Integrins $\alpha_v\beta_3$ and $\alpha_v\beta_5$ promote adenovirus internalization but not virus attachment. *Cell* 1993; **73**: 309–319.
8 Hedley SJ, Chen J, Mountz JD, Li J, Curiel DT, Korokhov N *et al*. Targeted and shielded adenovectors for cancer therapy. *Cancer Immunol Immunother* 2006; **55**: 1412–1419.
9 Taki M, Kagawa S, Nishizaki M, Mizuguchi H, Hayakawa T, Kyo S *et al*. Enhanced oncolysis by a tropism-modified telomerase-specific replication-selective adenoviral agent OBP-405 ('Telomelysin-RGD'). *Oncogene* 2005; **24**: 3130–3140.
10 Klionsky DJ, Cuervo AM, Seglen PO. Methods for monitoring autophagy from yeast to human. *Autophagy* 2007; **3**: 181–206.
11 Paglin S, Hollister T, Delohery T, Hackett N, McMahill M, Sphicas E *et al*. A novel response of cancer cells to radiation involves autophagy and formation of acidic vesicles. *Cancer Res* 2001; **61**: 439–444.
12 Mizushima N. Methods for monitoring autophagy. *Int J Biochem Cell Biol* 2004; **36**: 2491–2502.
13 Mizushima N, Yoshimori T. How to interpret LC3 immunoblotting. *Autophagy* 2007; **3**: 542–545.
14 Aoki H, Takada Y, Kondo S, Sawaya R, Aggarwal BB, Kondo Y. Evidence that curcumin suppresses the growth of malignant gliomas *in vitro* and *in vivo* through induction of autophagy: role of Akt and extracellular signal-regulated kinase signaling pathways. *Mol Pharmacol* 2007; **72**: 29–39.
15 Aoki H, Kondo Y, Aldape K, Yamamoto A, Iwado E, Yokoyama T *et al*. Monitoring Autophagy in Glioblastoma with Antibody against Isoform B of Human Microtubule-Associated Protein 1 Light Chain 3. *Autophagy* 2008; **4**: 467–475.
16 Klionsky DJ, Abeliovich H, Agostinis P, Agrawal DK, Aliev G, Askew DS *et al*. Guidelines for the use and interpretation of assays for monitoring autophagy in higher eukaryotes. *Autophagy* 2008; **4**: 151–175.
17 Tanida I, Minematsu-Ikeguchi N, Ueno T, Kominami E. Lysosomal turnover, but not a cellular level, of endogenous LC3 is a marker for autophagy. *Autophagy* 2005; **1**: 84–91.
18 Shintani T, Klionsky DJ. Autophagy in health and disease: a double-edged sword. *Science* 2004; **306**: 990–995.
19 Takeuchi H, Kondo Y, Fujiwara K, Kanzawa T, Aoki H, Mills GB *et al*. Synergistic augmentation of rapamycin-induced autophagy in malignant glioma cells by phosphatidylinositol 3-kinase/protein kinase B inhibitors. *Cancer Res* 2005; **65**: 3336–3346.
20 Kanzawa T, Germano IM, Komata T, Ito H, Kondo Y, Kondo S. Role of autophagy in temozolomide-induced cytotoxicity for malignant glioma cells. *Cell Death Differ* 2004; **11**: 448–457.
21 Giannini C, Sarkaria JN, Saito A, Uhm JH, Galanis E, Carlson BL *et al*. Patient tumor EGFR and PDGFRA gene amplifications retained in an invasive intracranial xenograft model of glioblastoma multiforme. *Neuro Oncol* 2005; **7**: 164–176.
22 Stupp R, Mason WP, van den Bent MJ, Weller M, Fisher B, Taphoorn MJ *et al*. Radiotherapy plus concomitant and adjuvant temozolomide for glioblastoma. *N Engl J Med* 2005; **352**: 987–996.

Supplementary Information accompanies the paper on Gene Therapy website (http://www.nature.com/gt)

Review Article

Understanding and exploiting *hTERT* promoter regulation for diagnosis and treatment of human cancers

Satoru Kyo,[1,3] Masahiro Takakura,[1] Toshiyoshi Fujiwara[2] and Masaki Inoue[1]

[1]Department of Obstetrics and Gynecology, Kanazawa University, Graduate School of Medical Science, 13-1 Takaramachi, Kanazawa, Ishikawa 920-8641; [2]Center for Gene and Cell Therapy, Okayama University Hospital, 2-5-1 Shikata-cho, Okayama 700-8558, Japan

(Received March 18, 2008/Revised April 23, 2008/Accepted April 23, 2008/Online publication July 29, 2008)

Telomerase activation is a critical step for human carcinogenesis through the maintenance of telomeres, but the activation mechanism during carcinogenesis remains unclear. Transcriptional regulation of the human telomerase reverse transcriptase (*hTERT*) gene is the major mechanism for cancer-specific activation of telomerase, and a number of factors have been identified to directly or indirectly regulate the *hTERT* promoter, including cellular transcriptional activators (c-Myc, Sp1, HIF-1, AP2, ER, Ets, etc.) as well as the repressors, most of which comprise tumor suppressor gene products, such as p53, WT1, and Menin. Nevertheless, none of them can clearly account for the cancer specificity of hTERT expression. The chromatin structure via the DNA methylation or modulation of nucleosome histones has recently been suggested to be important for regulation of the *hTERT* promoter. DNA unmethylation or histone methylation around the transcription start site of the *hTERT* promoter triggers the recruitment of histone acetyltransferase (HAT) activity, allowing *hTERT* transcription. These facts prompted us to apply these regulatory mechanisms to cancer diagnostics and therapeutics. Telomerase-specific replicative adenovirus (Telomelysin, OBP-301), in which *E1A* and *E1B* genes are driven by the *hTERT* promoter, has been developed as an oncolytic virus that replicates specifically in cancer cells and causes cell death via viral toxicity. Direct administration of Telomelysin was proved to effectively eradicate solid tumors *in vivo*, without apparent adverse effects. Clinical trials using Telomelysin for cancer patients with progressive stages are currently ongoing. Furthermore, we incorporated green fluorescent protein gene (*GFP*) into Telomelysin (TelomeScan, OBP-401). Administration of TelomeScan into the primary tumor enabled the visualization of cancer cells under the cooled charged-coupled device (CCD) camera, not only in primary tumors but also the metastatic foci. This technology can be applied to intraoperative imaging of metastatic lymphnodes. Thus, we found novel tools for cancer diagnostics and therapeutics by utilizing the *hTERT* promoter. (*Cancer Sci* 2008; 99: 1528–1538)

In the past decade, research in the field of telomerases has progressed tremendously, especially in relation to cellular immortality and carcinogenesis. Telomerase activation is observed in approximately 90% of human cancers, irrespective of tumor type, while most normal tissues contain inactivated telomerase.[1] The role and timing of telomerase activation in carcinogenesis has been revealed by telomerase-knockout mouse studies.[2,3] Significant telomere erosions and age- and generation-dependent increases in cytogenic abnormalities are exhibited in telomerase-knockout mice, providing evidence that telomere dysfunction with critically short telomeres causes genomic instability.[2] This concept is further supported by studies using telomerase–/– p53–/– double-knockout mice.[3] These mouse cells demonstrate high levels of genomic instability, exemplified by increases in both formation of dicentric chromosomes and susceptibility to oncogenic transformation. These mice exhibit significantly decreased tumor latency and overall survival. Thus, in the absence of genome checkpoint functions, telomere dysfunction accelerates genomic instability, facilitating cancer initiation.[4] According to this concept, the genomic instability caused by telomere dysfunction occurs in the early stages of carcinogenesis, before telomerase activation. Subsequently, telomeres in these initiated cells undergo further progressive shortening, generating rampant chromosomal instability and threatening cell survival. Telomerase activation necessarily occurs at this stage to stabilize the genome and confer unlimited proliferative capacity upon the emerging and evolving cancer cell. In other words, cells that have acquired telomerase activity can obtain the capacity for cancer progression. Eventually, most cancer cells exhibit telomerase activity.

This cancer-specific telomerase activity provides an opportunity for us to utilize it for cancer diagnosis and treatment. Continuous effort has been made to uncover the molecular mechanisms of telomerase activation during carcinogenesis. The discovery of the telomerase subunit human telomerase reverse transcriptase (hTERT),[5,6] a catalytic subunit bearing the enzymatic activity of telomerase,[7,8] was the starting point for uncovering the cancer-specific activation of telomerase. Numerous studies have demonstrated that hTERT expression is highly specific to cancer cells and tightly associated with telomerase activity, while the other subunits are constitutively expressed both in normal and cancer cells.[9–12] Therefore, there is no doubt that hTERT expression plays a key role in cancer-specific telomerase activation. In this review article, we discuss the cancer-specific regulation of *hTERT* and its application for cancer diagnosis and treatment.

Cloning of the *hTERT* promoter and identification of the core promoter region containing *cis*- and *trans*-elements for cancer-specific transcription

In 1999 we and other groups successfully cloned the 5′-promoter region of the *hTERT* gene.[13–15] Transient expression assays using the 3.0 kb of the flanking sequences of the *hTERT* gene revealed that the transcriptional activity was up-regulated

[3]To whom correspondence should be addressed.
E-mail: satoruky@med.kanazawa-u.ac.jp

doi: 10.1111/j.1349-7006.2008.00878.x

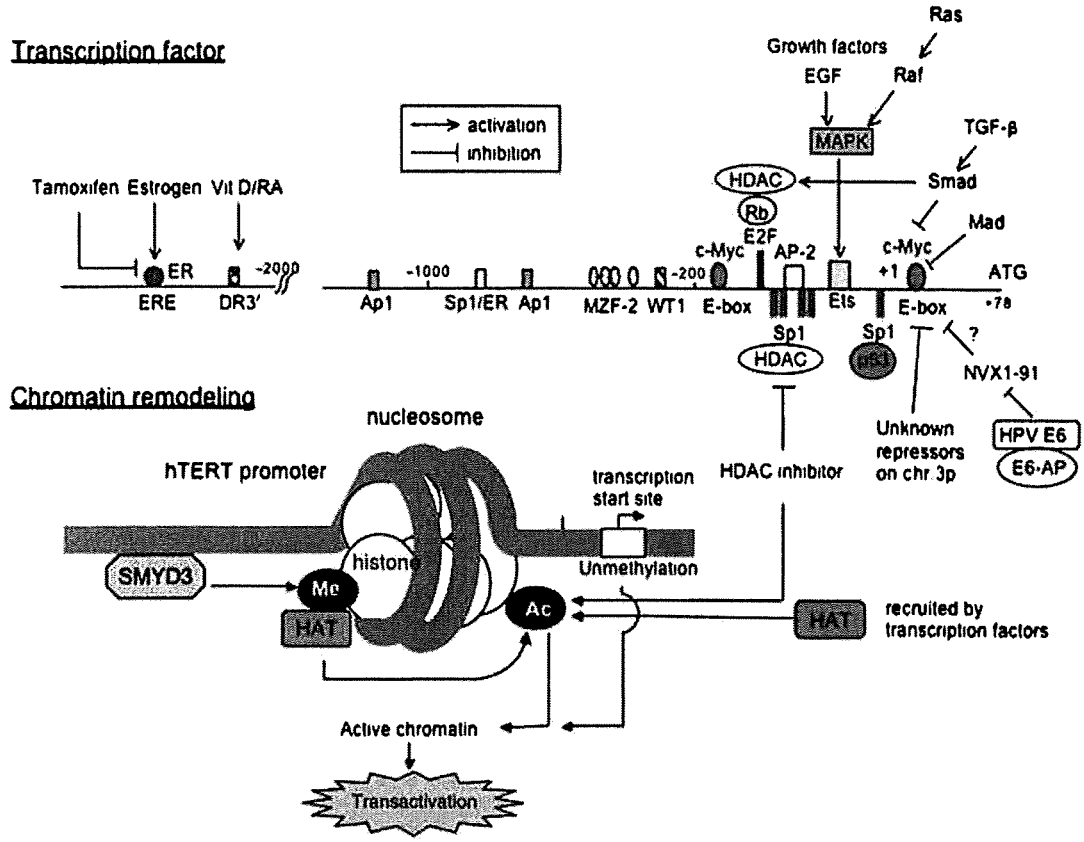

Fig. 1. Complex molecular mechanisms of transcriptional regulation of human telomerase reverse transcriptase (*hTERT*). Representative transcription factors and their upstream factors essential for *hTERT* regulation are shown in the upper panel. The sites on the promoter are not precisely in scale. +1 indicates the start site of transcription.[13] The proposed model of chromatin remodeling for the regulation of *hTERT* promoter is shown in the lower panel. Me, methylation of histone; Ac, acetylation of histone.

specifically in cancer cells, while it was silent in most normal cells.[13] Deletion analysis of the promoter identified the proximal 260 bp region functioning as the core promoter essential for cancer-specific transcriptional activation. Within the core promoter, several distinct transcription-binding sites are present; E-boxes (CACGTG) located at −165 and +44 (numbering based on the transcription start site determined by CapSite Hunting method[11]) are potential binding sites of basic helix-loop-helix zipper (bHLHZ) transcription factors encoded by the Myc family oncogenes. The existence of E-boxes on the *hTERT* promoter stirred telomerase researchers since c-Myc has been known to activate telomerase.[16] In fact, several groups confirmed that c-Myc binds to E-boxes on the *hTERT* promoter and activates the transcription[15–19] which established the scenario that c-Myc is a key regulator of *hTERT* transcription during carcinogenesis. However, several studies found that Myc and hTERT expression levels are not necessarily tightly correlated in some cancer cells.[20,21] Furthermore, it should be noted that most of these studies used overexpressed c-Myc for the luciferase reporter assay as well as recombinant c-Myc for the electrophoretic mobility shift assay (EMSA) to demonstrate binding to the E-boxes. Therefore, it remains unclear whether endogenous binding of c-Myc on the *hTERT* promoter plays a critical role in *hETRT* transcription *in vivo*, especially during carcinogenesis. Xu *et al.* reported the important finding that endogenous c-Myc binding to the E-boxes on the *hTERT* promoter was well correlated with the induction of *hTERT* in proliferating leukemic cells.[22] Nevertheless, it remains unclear whether up-regulation of *in vivo* binding of c-Myc to the *hTERT* promoter occurs during carcinogenesis and how critical it is for continuous hTERT expression in cancer.

Other characteristic sequences that exist on the *hTERT* promoter are the GC-boxes (GGGCGG), which are binding sites for zinc finger transcription factor Sp1. There are at least five GC-boxes within the core promoter of *hTERT*, proven by EMSA to bind Sp1.[22] Introduction of mutations in these GC-boxes significantly decreased the transcriptional activity of the promoter, while overexpression of Sp1 in cells that contain relatively low levels of endogenous Sp1 enhanced the promoter activity.[17] In particular, the *hTERT* core promoter activity was almost completely diminished by introducing mutations in all five GC-boxes, while mutation in one site moderately decreased it. Therefore, the GC-boxes function synergistically to maintain the promoter activity of *hTERT*. However, Sp1 is ubiquitously expressed in a wide range of normal cells, and is not therefore a strong candidate to cause cancer-specific hTERT expression.

Overall, while the *hTERT* core promoter is highly specific to cancer cells, the key transcription factors identified are far from accounting for cancer-specific *hTERT* expression.

Critical factors that regulate *hTERT* transcription

A number of factors that regulate *hTERT* transcription have been identified to regulate the *hTERT* promoter. The representative regulators of *hTERT* promoter with regard to the clinical aspects are shown in Fig. 1.

Cellular transcription factors. Several transcription factors, as well as c-Myc and Sp1, have been identified to regulate the *hTERT* promoter. Activating Enhancer-binding Protein-2 (AP-2) was recently identified as a transcriptional activator of the *hTERT* promoter[23] and, of particular interest, it exhibited tumor-specific

binding to the core promoter region. Although this study examined only one tumor type (lung cancer), this may partly explain tumor-specific *hTERT* transcription.

Hypoxia-inducible factor-1 (HIF-1), a key regulator of O_2 homeostasis, regulates the expression of several genes linked to angiogenesis and energy metabolism. The presence of putative HIF-1 binding sites on the *hTERT* promoter prompted us to examine the involvement of HIF-1 in regulation of *hTERT* in tumor hypoxia: we found that hypoxia activated hTERT mRNA in cancer cells *in vitro*.[24,25] Luciferase reporter assays revealed that *hTERT* transcription was significantly activated in hypoxia and by HIF-1α overexpression, and that the two putative HIF-1 binding sites within the core promoter are responsible for this activation. The chromatin immunoprecipitation assay identified specific binding of HIF-1α to these sites, which was enhanced in hypoxia. siRNA inhibition of HIF1-α abrogated hypoxia-induced hTERT mRNA expression. Thus, hypoxia activates telomerase mainly via transcriptional activation of *hTERT*, and HIF-1 plays a critical role as a transcription factor. In contrast to these findings, Koshiji *et al.* observed that HIF-1 inhibited *hTERT* expression in colon cancer cells.[26] In this study, they demonstrated that HIF-1 induces cell-cycle arrest even in the absence of hypoxia by functionally counteracting Myc. Eventually, HIF-1 down-regulates Myc-activated genes including *hTERT*. The reasons for this discrepancy remain unclear, but experimental conditions, such as the concentration of oxygen and constitutive levels of HIF-1 in cell types used, may significantly affect the results. A recent study underscored the importance of HIF-2 in regulating *hTERT* promoter.[27] While HIF2-α enhances *hTERT* expression in renal-cell carcinoma, it represses *hTERT* transcription in glioma cells, adding a further layer of complexity to the relationship between hypoxia and telomerase activity.

We also found the transcription activator protein AP-1 to function as a transcriptional repressor.[28] There are two AP-1 sites (at –1655 and –718) within the 2.0 kb promoter of *hTERT*. EMSA revealed that JunD is the major factor binding to them, which was further supported by chromatin immunoprecipitation (ChIP) assay *in vivo*. Overexpression of Jun family members with c-fos significantly reduced the promoter activity while mutation of AP-1 sites increased it. Of particular interest is the observation that AP-1 had no effect on the mouse *TERT* (*mTERT*) promoter although it has similar binding sites for AP-1. Since *mTERT* is constitutively expressed both in tumor and normal cells, this species-specific function of AP-1 in *TERT* expression may in part help explain the difference in telomerase activity between normal human and mouse cells.

Hormones. Hormonal regulation of *hTERT* and the molecular mechanisms involved have been analyzed most extensively in relation to estrogen. We and other groups found that estrogen activates *hTERT* transcription via binding of ligand-activated estrogen receptor-α (ERα) to the estrogen-responsible element (ERE) in the *hTERT* promoter.[29,30] ER-Sp1 half-sites located downstream of the ERE similarly function as *cis*-acting elements in response to estrogen stimulation. Estrogen also activates *hTERT* expression via post-transcriptional mechanisms with the stimulation of nuclear accumulation of hTERT via its phosphorylation, which is mediated by Akt signaling.[31] Tamoxifen, a selective estrogen receptor modulator, also regulates *hTERT* expression in a cell-type-specific manner;[32] tamoxifen inhibits the growth of breast cancer cells, as well as hTERT mRNA expression in the presence of estrogen (E2), antagonizing the E2 effects, in which the ERE on the promoter is involved. In contrast, tamoxifen stimulated the growth of endometrial cancer cells and activated hTERT mRNA expression in the absence or presence of E2, exhibiting estrogen-agonistic action, in which MAP kinase signaling pathways are involved. Androgen was also shown to activate hTERT mRNA in androgen-sensitive prostate cancer cells but this regulation was not due to *hTERT* promoter activation.[33] Progesterone exerts diverse effects on hTERT mRNA expression in a time-dependent manner in progesterone-receptor-positive breast cancer cells;[34] in the short term, it activates *hTERT* transcription, but prolonged exposure to progesterone antagonizes estrogen and inihibits *hTERT* transcription. Interestingly, both short- and long-term regulation is mediated via the MAP kinase signaling pathway.

Cytokines. Telomerase activation is known to be tightly associated with cell proliferation, which suggests that growth signaling might directly regulate hTERT expression.[35–37] We established an *in vitro* model in which telomerase activity can easily be induced upon stimulation of EGF in EGF-receptor-positive cancer cells.[38] Luciferase reporter assays revealed that EGF activates the *hTERT* promoter: an Ets motif located in the core promoter of *hTERT* is responsible. Notably, MAP kinase signaling pathways mediate this regulation. A number of growth signals have been known to be mediated through MAP kinase pathway, with Ets factors playing critical roles as final mediators regulating the target-gene expression. Therefore, EGF-mediated Ets-based *hTERT* transcription may be one representative pathway through which various growth signals are transduced to the *hTERT* promoter. This scenario can partly account for telomerase activation associated with cell proliferation.

TGF-β is a representative cytokine that represses *hTERT* transcription.[39] The mechanisms through which TGF-β down-regulates *hTERT* transcription are controversial: while some studies demonstrated that TGF-β repressed *hTERT* transcription via indirect down-regulation of c-Myc expression,[40,41] others reported direct interaction of Smad3 and c-Myc disturbing c-Myc activity.[42] Another study identified several negative regulatory factors for *hTERT* by means of gene screening using enhanced retroviral mutagenesis (ERM) and found that Smad interacting protein-1 (SIP1) is a repressor for *hTERT*, possibly mediating TGF-β signals.[43] A more recent study using siRNA inhibition of the Smad family confirmed that TGF-β-mediated repression of *hTERT* transcription is largely mediated through Smad3, not Smad1 or Smad2.[44] However, this study found no role for E-boxes in this repression, but found four E2F-binding sites within the proximal promoter of *hTERT* to be responsible, based on the data that mutation of these four sites reversed TGF-β-mediated repression of *hTERT* transcription. The transcriptional activity of E2F family members is regulated by interactions with pocket proteins (Rb, p107, p130) that recruit histone deacetylase (HDAC) proteins to repress target genes. Interestingly, overexpression of the dominant negative E2F gene lacking the ability to bind pocket protein (Rb, p107, p130) and to recruit HDAC significantly abrogated TGF-β-mediated repression of *hTERT* transcription. Furthermore, trichostatine A (TSA), a HDAC inhibitor, completely reversed the inhibitory effect of TGF-β. These findings highlight E2F and HDAC as central mediators of TGF-β-mediated repression of *hTERT* transcription. The involvement of HDAC in *hTERT* transcription is also discussed below.

Oncogenes. High-risk human papillomaviruses (HPV) are representative oncoviruses whose E7 protein can bind to Rb and alleviate repression of E2F-dependent target genes, thereby allowing rapid progression into S phase[45] while E6 protein facilitates the degradation of p53 through the actions of E6-associated protein (E6-AP), which results in the abrogation of the G_1/S and G_2/M checkpoints.[46–48] The initial study found that telomerase is activated in keratinocytes stably expressing HPV16 E6.[49] Since E6 had been known to activate c-Myc expression[50] it seemed likely that E6 activates *hTERT* transcription via up-regulating c-Myc. However, subsequent studies confirmed that high-risk HPV E6 activates *hTERT* transcription but is not associated with up-regulation of c-Myc.[51–53] Several studies found that *hTERT* transactivation by HPV16 E6 correlates with its ability to bind E6-AP.[54] A correlation between E6-AP binding and *hTERT* induction prompted the search for possible targets of

doi: 10.1111/j.1349-7006.2008.00878.x

the E6/E6-AP complex by a yeast two-hybrid screen, which identified a transcriptional repressor known as NFX1 that binds to 48-bp sequences surrounding the proximal E-box on the *hTERT* promoter.[54] It is supposed that the E6/E6-AP complex induces hTERT expression by destabilizing NFX-1. In support of this, decreased expression of NFX1 using siRNAs was sufficient to induce *hTERT* expression and telomerase activity in primary human epithelial cells.

Some human oncoproteins specifically activate *hTERT* promoter. In hTERT-negative normal cells, HER2/Neu signals (by overexpressing oncogenic HER2/Neu mutant) alone failed to activate the endogeneous *hTERT* expression.[55] However, coexpression of HER2/Neu with one ETS family member (ER81) successfully activated *hTERT* expression in these cells. There are five putative binding core GGAA/T sites for ETS family in exon1 to intron1 of the *hTERT* gene, and ER81 specifically binds to two of them and activates *hTERT* promoter in cooperation with HER2/Neu signals. Notably, this activation was mediated via the ERK-MAP kinase pathway, in which upstream Ras and Raf-1 play critical roles. Thus, three prominent oncoproteins, HER2/Neu, Ras, and Raf, facilitate *hTERT* expression via an Ets family member in hTERT-negative normal cells.

Epigenetic regulation of *hTERT* transcription

The *hTERT* promoter contains a cluster of CpG sites, and many researchers therefore supposed its regulation to involve DNA methylation. Several groups examined the methylation status of these CpG sites on this promoter. It was initially expected that methylation of the *hTERT* promoter was associated with gene silencing; indeed, some groups showed such association.[56–58] However, other reports indicated no significant correlation between *hTERT* expression and methylation status either overall or at a specific site.[59,60] Furthermore, contradictory results have been reported: increased DNA methylation in the *hTERT* promoter was observed in hTERT-positive cancer cells while lack of methylation was found in normal hTERT-negative cells.[61] These unusual correlations between DNA methylation and hTERT expression in normal and cancer cells generated confusion among telomerase researchers. Recently, Zinn *et al.* aimed to clarify the discrepancies:[62] using bisulfite sequencing, they first identified that all telomerase-positive cancer cell lines examined retained alleles with little or no methylation around the transcription start site despite being densely methylated in more upstream regions. ChIP assay revealed that both active (acethyl-H3K9 and dimethyl-H3K4) and inactive (trimethyl-H3K9 and trimethyl-H3K27) chromatin marks are present across the *hTERT* promoter. Subsequent Chip-MSP (methylation-specific polymerase chain reaction [PCR]) assay identified that active chromatin mark DNA around the transcription start site was tightly associated with unmethlated DNA. These data suggest that the absence of methylation and the association with active chromatin marks around the transcription start site allow for the expression of *hTERT* (Fig. 1), indicating that the DNA methylation pattern of the *hTERT* promoter is consistent with the usual dynamics of gene expression.

Modification of nucleosome histones, including acetylation/deacetylation as well as methylation, is known to regulate chromatin structure and thereby affect gene transcription.[63] Roles for histone-modification-mediated chromatin remodeling in the regulation of *hTERT* transcription have been revealed (Fig. 1). We and other groups found that treatment with TSA induced significant elevation of hTERT mRNA expression and telomerase activity in normal cells, but not in cancer cells.[64,65] Transient expression assays revealed that TSA activates the *hTERT* promoter, for which the proximal core promoter was responsible. Overexpression of Sp1 enhanced responsiveness to TSA, and mutation of Sp1 sites but not c-Myc sites of the core promoter of *hTERT* abrogated this activation. Introduction of the dominant-negative form of the Sp family inhibited TSA activation. These results indicate that HDAC inhibitor activates the *hTERT* promoter in normal cells in an Sp1-dependent manner (Fig. 1). It is possible that endogeneous Sp1 interacts with HDAC and recruits it to the *hTERT* promoter[66] resulting in the deacetylation of nucleosome histones, leading to the repression of transcription. While Sp1 contributes to the transactivation of *hTERT* as a potent transcriptional activator[22] it might be involved in gene silencing of *hTERT* in normal cells, possibly by recruiting HDACs. Compelling evidence suggests that Sp1 interacts with a p300 coactivator possessing intrinsic histone acetyltransferase (HAT) activity.[67] Therefore, it is possible that Sp1 interacts with various factors that have HAT or HDAC activity, and that this switching explains the different actions of Sp1 on the *hTERT* promoter in normal and cancerous cells. The E-box binding activator c-Myc and repressor Mad1[21,22,68] which compete with each other for the common binding partner Max are also involved in histone-modification-mediated chromatin remodeling of the *hTERT* promoter. The endogenous c-Myc/Max complex to the *hTERT* promoter in proliferating leukemia cells was found to be associated with the acetylated histones, resulting in enhanced hTERT expression.[22] In contrast, the complex was replaced by the endogeneous Mad1/Max complex that was associated with deacetylated histones and decreased *hTERT* expression in differentiated status.

Recently, a role for histone methylation in *hTERT* regulation has also been demonstrated. Atkinson *et al.* observed that highly trimethylated H3-K4 was associated with the actively transcribed *hTERT* gene in telomerase-proficient tumor cells.[69] More recently, we reported the interesting finding that SET- and MYND-domain-containing protein-3 (SMYD3), a histone H3-K4-specific dimethyltransferase and trimethyltransferase, respectively, play critical roles in H3-K4 methylation of the *hTERT* promoter.[70] Of the various SET-domain-containing proteins, SMYD3 is unique because not only does it have methyltransferase activity but it also binds to a specific DNA sequence (CCCTCCC) in its target promoters, as do transcription factors. In fact, SMYD3 was confirmed to bind some of the CCCTCCC motifs within the core promoter of *hTERT* and activate *hTERT* transcription. Overexpression of *SYND3* induced hTERT mRNA expression in hTERT-negative normal and cancer cells. Disruption of SMYD3 binding motifs in the *hTERT* promoter led to significant reduction of transcription. Expectedly, siRNA-knockdown of *SMYD3* resulted in abolishment of H3-K4 trimethylation of the *hTERT* promoter in cancer cells; interestingly, this knockdown also led to defects in binding c-Myc and Sp1. Furthermore, histone H3 acetylation within the core promoter of *hTERT* was diminished by the *SMYD3*-knockdown. These data suggest a model in which SMYD3 binding to the *hTERT* promoter leads to increased H3 trimethylation, a critical event that recruits HAT and promotes Sp1 and c-Myc access to the *hTERT* promoter (Fig. 1). Thus, SMYD3-mediated trimethylation of H3-K4 may function as a licensing element for subsequent transcription-factor binding to the *hTERT* promoter, which may trigger further recruitment of HAT activity.

Identification of *hTERT* repressors

Recently, Lin *et al.*[43] identified several negative regulatory factors for *hTERT* by means of gene screening that used enhanced retroviral mutagenesis (ERM). They identified menin, SIP1, Mad1, hSIR2, and BRIT1 as candidates for the *hTERT* repressor, generating the idea that multiple tumor suppressors might involve telomerase repression, especially in normal cells. p53 was also shown to repress *hTERT* transcription in a Sp1-dependent manner.[71,72] It was proved that p53 can form a complex with Sp1, which disturbs the transcriptional activity of Sp1 and leads to transcriptional repression.[72] Several transcriptional repressors,

including Wilms' tumor 1 tumor suppressor (WT1) and myeloid-specific zinc finger protein-2 (MZF-2) are also known to repress *hTERT* transcription via binding to their specific sites on the promoter, although the mechanisms of repression remain unclear.[73,74] We also found that on combinatorial treatment with Vitamin D3 and 9-*cis*-retinoic acid, the heterodimer complex, vitamin D[3] receptor/retinoid X receptor (RXR), binds to the distal sites on the *hTERT* promoter and represses transcription.[75]

There has been an extensive search for telomerase repressors, one of which was based on microcell-mediated chromosome transfer.[76] Several normal human chromosomes, including chromosomes 3, 4, 6, 7, 10, and 17, have been shown to repress telomerase activity in some but not all cancer cells.[77–85] Horikawa *et al.* established a nice system to investigate an endogenous mechanism for telomerase repression using a telomerase-positive renal carcinoma cell line (RCC23) and telomerase-negative counterpart (RCC23 + 3) generated by transferring a normal chromosome 3 into RCC23 cells.[86] By comparing the molecular characteristics of these cells, they identified the E-box downstream of the transcription initiation site that was responsible for telomerase repressive mechanisms restored by normal chromosome 3 targets. They also found that the factors binding to the E-box, other than c-Myc/Mad or USF families, were involved in the transcriptional repression of *hTERT* although they remained to be cloned. This E-box-mediated repression functions in various types of normal human cells, while it is inactive in some, but not all, hTERT-positive cancer cells, providing evidence for an endogenous mechanism for *hTERT* transcriptional repression that becomes inactivated during carcinogenesis.

hTERT promoter for cancer therapeutics

***hTERT* promoter for cancer-specific transgene expression.** In the field of cancer gene therapy, the researchers have a great interest in efficiently expressing target genes in the tumor tissue while decreasing adverse effects in normal tissue. Control of gene expression via tissue- or cell-specific promoters has been tested extensively as a means of targeting transgene expression. Several promoters have been identified that are more active in particular tumor types than in the tissues from which they arise, and these promoters have been exploited to target transgene expression in tumors. These promoters include the tyrosinase gene promoter in melanomas,[87] the carcinoembryonic antigen promoter in colorectal and lung cancer,[88] the MUC1 promoter in breast cancer,[89] and the E2F promoter in cancers that carry a defective retinoblastoma gene.[90] However, while reports on these promoters suggest that achieving relatively tumor-specific transgene expression is possible, several limitations have also been revealed. First, most of these promoters are limited to specific tumor histologies and cannot be used universally in tumors of various origins. Second, most of these promoters are much weaker than commonly used viral promoters such as the CMV early promoter, the Rous sarcoma virus long-terminal repeat (RSV-LTR), and the SV40 early promoter. Consequently, their use is hampered by the problem of low expression.

The *hTERT* promoter is ideal to overcome the shortcoming of these promoters. Gu *et al.* first established the binary adenoviral system, which uses two adenoviral vectors to induce *Bax* gene expression.[91] One of these vectors contains a human *Bax* cDNA under the control of a minimal synthetic promoter comprising five Gal-4-binding sites and a TATA box, which is silent in 293 packaging cells, thus avoiding the toxic effects of the *Bax* gene on the 293 cells and allowing vector (Ad/GT-Bax) production. Expression of the *Bax* gene can be induced by coinfecting the Ad/GT-Bax virus with the second adenoviral vector in the binary system (Ad/PGK-GV16), which consists of a fusion protein comprising a Gal-4 DNA-binding domain and a VP 16 activation domain under the control of a constitutively active PGK promoter. Ad/PGK-GV16 is expected to produce VP16 with Gal-4 DNA binding domain preferentially in tumor cells and thereby induce *Bax* gene expression via interaction with Gal-4-binding sites. This binary infection system was reported to suppress tumor growth *in vitro* and *in vivo*. More simple vector systems to achieve cancer-specific transgene expression have been tried, in which several apoptosis-inducible genes such as *FADD*,[92,93] *caspace*[94,95] or suicide gene (human herpes simplex virus thymidine kinase (*HSVtk*) gene),[96] tumor-necrosis-factor-related apoptosis-inducing ligand gene (*TRAIL*),[97] or chemoattractant protein gene (*MCP-1*)[98] have been driven by the *hTERT* promoter in various tumor types. Most of these studies successfully demonstrated tumor-specific transgene expression *in vivo*, achieving long-term survival benefit and minimizing its expression in normal tissues following direct injection of the vectors and even with systemic injection. Systemic toxicity is one concern in this treatment modality because telomerase activity has been reported to exist in some normal cells, such as hematopoietic crypt and endometrial cells, most of which have high regenerative potentials. Gu *et al.* tested *hTERT*-promoter-driven transgene expression in human CD34(+) bone marrow progenitor cells and found very low *hTERT* promoter activity in these cells as well as no detectable change in blood-cell profiles under long-term observation.[99] Basically, the *hTERT* promoter activity in these normal cells with telomerase activity is much lower than that in cancer cells, and toxicity is expected to be minimized.

***hTERT* promoter for cancer-specific replication-competent adenovirus.** Despite these efforts, levels of transgene expression were insufficient to eradicate tumors, especially when vectors were systemically administrated. This is mainly due to the characteristics of adenoviral vectors used, in which the *E1* gene was deleted to inhibit replicative capacity. These nonreplicative vectors had limited distribution within the tumor mass even after direct intratumoral administration. To confer specificity of infection and increase viral spread to neighboring tumor cells, the use of replication-competent adenoviruses has become a reality. The use of modified adenoviruses that replicate and complete their lytic cycle preferentially in cancer cells is a promising strategy for the treatment of cancer. Many efforts have been made to realize cancer-specific adenoviral replication using a variety of gene promoters, including the prostate-specific antigen,[100] MUC1,[101] osteocalcin,[102] L-plastin,[103] midkine,[104] and *E2F-1* genes.[105] Unfortunately, these promoters have tissue-type specificity and exhibit transcriptional activity only in cells that express such tumor markers. Furthermore, the transcriptional activity is relatively low. We were prompted by these studies to use the *hTERT* promoter, hypothesizing that an adenovirus containing the *hTERT* promoter-driven *E1* genes could target a variety of tumors and kill them with high replicative capacity.

We developed a novel telomerase-dependent replicative adenovirus type 5 vector (Telomelysin, OBP-301) in which *E1A* and *E1B* genes, required for adenoviral replication, were transcribed under the *hTERT* promoter.[106] In most vectors that replicate under the transcriptional control of the *E1A* gene, *E1B* is driven by the endogeneous adenovirus *E1B* promoter. However, the insertion of internal ribosome entry site (IRES) between *E1A* and *E1B* improved the promoter specificity of *E1B* transcription. We selected the 455 bp-proximal promoter region of the *hTERT* gene to drive *E1A* and *E1B* genes because our previous experiments showed that this region exhibits the highest transcriptional activity, comparable to the proximal core promoter.[13] The construction of Telomelysin is shown in Fig. 2. Similar replicative adenoviruses controlled by the *hTERT* promoter have also been developed by other groups.[107–109]

In vitro replication assays revealed that Telomelysin induced selective expression of *E1A* and *E1B* in cancer cells, resulting in viral replication at 5–6 orders of magnitude by 3 days after infection, while it was attenuated by up to 2 orders of magnitude

doi: 10.1111/j.1349-7006.2008.00878.x